**11 Rapid #: -1807965**

**Ariel IP: 18.51.0.167**

| Status | Rapid Code | Branch Name | Start Date |
|---|---|---|---|
| Pending | LHL | Main Library | 5/13/2008 9:43:57 AM |

**CALL #:** **Applied magnetic resonance.**

**LOCATION:** **LHL :: Main Library :: Linda Hall Library - closed stacks**

| | |
|---|---|
| TYPE: | Article CC:CCG |
| JOURNAL TITLE: | Applied magnetic resonance |
| USER JOURNAL TITLE: | Applied Magnetic Resonance |
| LHL CATALOG TITLE: | Applied magnetic resonance. |
| ARTICLE TITLE: | A Closer look at Photochemical Reactions of Transition Metal Compounds using time resolved EPR |
| ARTICLE AUTHOR: | Martino D |
| VOLUME: | 26 |
| ISSUE: | |
| MONTH: | |
| YEAR: | 2004 |
| PAGES: | 489-519 |
| ISSN: | 0937-9347 |
| OCLC #: | |
| CROSS REFERENCE ID: | 111005 |
| VERIFIED: | |

**BORROWER:** **MYG :: Main Library**

**PATRON:** **martino,Debora**

| | |
|---|---|
| PATRON ID: | |
| PATRON ADDRESS: | |
| PATRON PHONE: | |
| PATRON FAX: | |
| PATRON E-MAIL: | dmartino@mit.edu |
| PATRON DEPT: | CHEM |
| PATRON STATUS: | VS |
| PATRON NOTES: | |

RAPID ILL


System Date/Time: 5/13/2008 12:20:05 PM MST

Appl. Magn. Reson. 26, 489–519 (2004)

**Applied Magnetic Resonance**



# A Closer Look at Photochemical Reactions of Transition-Metal Compounds by Time-Resolved EPR

**D. M. Martino[1,2], C. J. Kleverlaan[3], J. van Slageren[4], A. Bussandri[1], H. van Willigen[1], and C. Kiarie[1]**

[1] Chemistry Department, University of Massachusetts at Boston, Boston, Massachusetts, USA
[2] Departamento de Física, Facultad de Bioquímica y Ciencias Biológicas, and Instituto de Desarrollo Tecnológico para la Industria Química, Consejo Nacional de Investigaciones Científicas y Técnicas, Universidad Nacional del Litoral, Santa Fe, Argentina
[3] Academic Center for Dentistry Amsterdam, Amsterdam, The Netherlands
[4] Physikalisches Institut, Universität Stuttgart, Stuttgart, Germany

Received February 2, 2004

**Abstract.** A review is given of applications of time-resolved electron paramagnetic resonance (TREPR) in the field of photochemistry of transition-metal compounds. The two main TREPR techniques used in these studies are described. A brief overview is given of chemically induced dynamic electron polarization mechanisms that can affect TREPR spectra and that can give insights into the mechanism of photochemical reactions. Following these background sections, experimental results are presented. The discussion focuses in particular on the Fourier-transform EPR studies of photoinduced metal-alkyl bond homolysis reactions of a series of transition-metal (Co, Ru, Re, Pt) complexes carried out by the authors.

## 1 Introduction

### *1.1 General Background*

Given that photochemical reactions in many cases involve paramagnetic intermediates, it is evident that electron paramagnetic resonance (EPR) can be an important source of information on processes that are of current interest. However, generally the lifetime of these intermediates is quite short so that the application of special methods of detection is required. For this purpose, a number of time-resolved EPR (TREPR) techniques with which the evolution of pulsed laser-generated paramagnetic species can be monitored with nanosecond time resolution have been developed [1–4]. Also, theories for the quantitative interpretation of time profiles of resonance signals given by transient free radicals have been formulated and make it possible to use TREPR to get detailed information on reaction mechanisms and dynamics [3, 5–7]. Among the methods used,

Fourier-transform EPR (FTEPR) [2, 8–11] has proven to be particularly well suited for the detection of short-lived free radicals formed in photochemical reactions since the method combines high spectral resolution with high sensitivity. Furthermore, when pulsed methods are used to generate the EPR spectra, the analysis of time profiles of resonance peaks becomes simpler than when time-resolved continuous-wave (cw) EPR is used.

In terms of time resolution, TREPR resembles other nanosecond time-resolved spectroscopic methods, such as time-resolved infrared (TRIR) and transient UV/Vis absorption spectroscopy, in which the spectrum from a species generated by pulsed laser excitation is monitored over time. However, a number of unique features make EPR a source of data that complement the information provided by optical spectroscopy. For instance, clearly only paramagnetic species contribute to the spectra. This, together with the (typically) small resonance line widths in spectra of organic free radicals, generally leads to well-resolved relatively simple spectra. Information on electron spin-nuclear spin hyperfine coupling constants (hfccs) and $g$-values derived from the spectra makes it possible to identify the paramagnetic molecules unequivocally [7]. The fact that signal contributions from different species can be resolved and identified facilitates the extraction of kinetic data from the time profiles of signal intensities. The spectral parameters ($g$-value, hfccs, line width) are also sensitive to intermolecular interactions and can serve, for instance, to get an insight into the spatial location of paramagnetic species in microheterogeneous environments [10].

Probably the most remarkable and valuable attribute of TREPR spectra is that the time profiles not only reflect chemical kinetics but also are strongly affected by chemically induced dynamic electron polarization (CIDEP) [3, 4, 12, 13]. CIDEP effects arise because the spin state populations of free radicals formed in a chemical reaction will initially not be at thermal equilibrium. Consequently, a TREPR spectrum acquired at a time $\tau_d$ after laser excitation of the sample will display anomalous signal intensities reflecting the non-Boltzmann spin distribution if $\tau_d$ is of the order of, or shorter than, the electron spin-lattice relaxation time $T_1$. CIDEP gives rise to enhanced absorption and/or stimulated emission peaks and has its origin in the spin selectivity of chemical and physical processes involved in free radical formation and decay [3, 4, 10, 12]. For this reason, TREPR studies can provide unique insights into the photophysics and -chemistry of free radical formation.

TREPR has been applied almost exclusively in investigations concerned with organic photochemistry [3, 4, 10, 11]. Transient paramagnetic species produced by photochemical reactions of transition-metal complexes in many cases cannot be detected with TREPR techniques because incomplete averaging of $g$ and hyperfine anisotropies as well as short spin-lattice relaxation times broaden resonance peaks beyond detection. Short relaxation times also may preclude the generation of observable CIDEP effects. Even so, the relatively few published studies that deal with the photochemistry of transition-metal complexes show that CIDEP effects can be much more strongly affected by minor variations in molecular structure and reaction conditions than is the case for organic photochem-

istry [11]. This must stem f
tronic states are typically c
ture or solvent-solute inter
istics of the reactive electr
a significant source of info
pounds.

Previous investigations
cleavage of a Co-$CH_3$ bond
of research and revealed so
series of FTEPR studies ha
of the transition-metal com
[Ru($CH_3$)($SnPh_3$)($CO)_2$(iPr-
methyl, ethyl, isopropyl or
DAB is $N,N'$-diisopropyl-1
that TREPR measurements
time-resolved spectroscopic
mechanism of photochemi

The discussion focuses pri
in our laboratories. Instrum
2. This will be followed by
a role. As noted above, a
provide information on the
cal reactions [1–4]. Detaile
spin polarization can be f
13]. Here only a brief su
obtained in the study of t
tions concerned with the in
by a discussion of experin
TREPR research can be f

*2.1 Ra*

Commercial cw EPR spec
and do not have the time
spin dynamics associated
detection method" [1, 3, 4
moved into the nanosecon
review, the signal from th

istry [11]. This must stem from the fact that in organometallics a variety of electronic states are typically closely spaced so that minor changes in ligand structure or solvent-solute interaction can have a significant effect on the characteristics of the reactive electronic state. Detailed TREPR studies, therefore, can be a significant source of information on the photochemistry of this class of compounds.

Previous investigations dealing with methyl radical formation by photoinduced cleavage of a Co-$CH_3$ bond demonstrated that TREPR can be applied in this field of research and revealed some interesting novel CIDEP effects [14, 15]. Also, a series of FTEPR studies have been carried out on the bond homolysis reactions of the transition-metal complexes [Re(R)$(CO)_3$(dmb)], [Ru(I)(R)$(CO)_2$(iPr-DAB)], [Ru$(CH_3)$(Sn$Ph_3$)$(CO)_2$(iPr-DAB)] and [Pt$(CH_3)_4$(iPr-DAB)] [16–20]. Here R is methyl, ethyl, isopropyl or benzyl, dmb is 4,4′-dimethyl-2,2′-bipyridine and iPr-DAB is *N*,*N*′-diisopropyl-1,4-diazabutadiene. Results of the measurements show that TREPR measurements can provide data that complement those given by other time-resolved spectroscopic techniques and contribute to the understanding of the mechanism of photochemical radical formation in transition-metal compounds.

### *1.2 Scope of Review*

The discussion focuses primarily on results obtained in investigations carried out in our laboratories. Instrumental aspects of this work will be summarized in Sect. 2. This will be followed by a discussion of the CIDEP mechanisms that can play a role. As noted above, a unique aspect of TREPR measurements is that they provide information on the role played by electron and nuclear spins in chemical reactions [1–4]. Detailed discussions of the various mechanisms that produce spin polarization can be found in a number of previous reviews [1, 3, 4, 10–13]. Here only a brief summary of CIDEP mechanisms relevant to the results obtained in the study of the transition-metal complexes will be given. The sections concerned with the instrumental and theoretical background will be followed by a discussion of experimental results. Reviews of advances in other areas of TREPR research can be found in recent publications [1–4, 21–23].

## 2 Instrumental Aspects

### *2.1 Radical Detection and Identification*

Commercial cw EPR spectrometers [7] have a time response of about 0.1 ms and do not have the time resolution required for studies of the chemical and spin dynamics associated with photochemical reactions. However, by the "direct detection method" [1, 3, 4] the time response of a cw EPR instrument can be moved into the nanosecond domain. In what will be labeled cw TREPR in this review, the signal from the microwave detector is directly routed to a boxcar

integrator (or other time-resolved data acquisition device). In this way, the spectrum of a transient species can be recorded by setting the detection window at a specific time relative to the laser excitation pulse and sweeping the magnetic field. Alternatively, the time profile of a peak in the spectrum can be recorded by sweeping the detection window for a fixed magnetic field setting. The cw TREPR method has a time resolution in the nanosecond range [24]. Detailed discussions of the cw TREPR technique can be found in the literature [1, 3, 4, 7, 24].

Time-resolved measurements with higher sensitivity and spectral resolution became possible with the introduction of pulsed EPR instruments [1, 8–10, 25]. In this case, the analysis of the time evolution of signal intensities also is simplified by the fact that it is not affected by the continuous presence of a microwave field, as is the case in cw TREPR measurements. Since this review primarily involves the application of FTEPR, salient features of this technique are presented below.

### *2.2 FTEPR*

The concept of FTEPR is identical to FTNMR (nuclear magnetic resonance) (or pulsed NMR) [26]. Detailed descriptions of pulsed EPR instruments have been published [8, 25]. In studies of transient free radicals, the sample is excited by a laser pulse and at a selected time $\tau_d$ after this pulse a $\pi/2$ microwave pulse is given. This causes a rotation of the magnetization vector from the $z$-axis (the direction of the external magnetic field) into the $xy$-plane. Following the microwave pulse, the resulting free induction decay (FID) signal given by the transverse magnetization is recorded. The FID represents the time domain spectrum of the radical(s) present at the time of the microwave pulse. Fourier transformation gives the frequency domain spectrum of the paramagnetic species present at $\tau_d$ [2, 10, 22, 25, 27]. By recording the FIDs for a series of delay times, the time evolution of the spectra can be monitored. Radicals formed after delivery of the microwave pulse do not contribute to the FID. Radical decay during FID acquisition shows up in the form of line broadening in the frequency domain spectrum.

Of critical importance for applications in photochemistry is that laser and microwave pulse widths typically fall in the 5 to 20 ns range and that the detection dead time sets the lower limit of the FID signal time to 50–100 ns. As a consequence, free radicals with lifetimes in excess of about 50 ns can be monitored with a time resolution in the nanosecond range. These operating parameters are similar to those of other nanosecond time-resolved spectroscopic techniques.

A comparison of cw TREPR and FTEPR techniques shows that each has distinct strengths and weaknesses. Because of the reduction in sensitivity, cw TREPR in most cases requires signal enhancement provided by CIDEP. Furthermore, the analysis of signal time profiles measured with the cw technique must



take into account the effect
in the interval between crea
other things, this gives rise
the spectral resolution that
second time domain. By co
mum spectral resolution un
of time profiles of signal i
represent the evolution of
tration. However, FTEPR h
by the $\pi/2$ microwave pulse
than the spectral width. To
formed at a series of fixed
from the discrete frequenc
protect the detection circuit
ment cannot be started un
chemical decay or short rela
this dead time, the radicals
tems that give broad peaks
with FTEPR. Since cw TR
suited for the study of tran
line spectra.

Spin systems of photochem
rium at the time of formati
electron spin polarization a
CIDEP mechanisms relevan
transition-metal complexes
the theoretical details of th
can be found in the literat

TM CIDEP can be exhibit
reactant molecule in the p
trated in Fig. 1. Photoexcit
intersystem crossing (ISC)
of the ISC process gives r
$T_{-1}$ spin states and produc
is fast enough to compete
the spin polarization is ca
triplets giving $\alpha$ and $\beta$ spi

take into account the effect of the microwave field on the spin state evolution in the interval between creation of the spin system and signal detection. Among other things, this gives rise to an off-resonance signal contribution that limits the spectral resolution that can be attained with delay time settings in the nanosecond time domain. By comparison, FTEPR offers higher sensitivity and optimum spectral resolution unaffected by delay time setting. Quantitative analysis of time profiles of signal intensities is facilitated by the fact that they simply represent the evolution of the product of spin polarization and radical concentration. However, FTEPR has its own limitations. First, the bandwidth covered by the $\pi/2$ microwave pulse (about 100 MHz) in many cases is substantially less than the spectral width. To overcome this limitation, measurements must be performed at a series of fixed fields so that the complete spectrum can be assembled from the discrete frequency ranges covered at these field settings. Second, to protect the detection circuit from the strong microwave pulse, the FID measurement cannot be started until 50–100 ns after the microwave pulse. If due to chemical decay or short relaxation times the signal decays into the baseline during this dead time, the radicals cannot be detected. In practice, this means that systems that give broad peaks (typically more than about 2 G) cannot be studied with FTEPR. Since cw TREPR does not suffer from this limitation, it is better suited for the study of transient paramagnetic molecules that give rise to broadline spectra.

## 3 CIDEP Mechanisms

Spin systems of photochemically generated radicals are not at thermal equilibrium at the time of formation [12]. Processes that give rise to a non-Boltzmann electron spin polarization are known as CIDEP mechanisms. An outline of the CIDEP mechanisms relevant for the interpretation of data obtained in studies of transition-metal complexes will be given below. The discussion will not go into the theoretical details of the effects, in-depth discussions of CIDEP mechanisms can be found in the literature [12, 13, 28–31].

### *3.1 Triplet Mechanism (TM)*

TM CIDEP can be exhibited by free radicals produced in a reaction involving a reactant molecule in the photoexcited triplet state [29, 30]. Its origin is illustrated in Fig. 1. Photoexcitation to a singlet excited state ($^1MX^*$) is followed by intersystem crossing (ISC) to a triplet excited state ($^3MX^*$). The spin selectivity of the ISC process gives rise to distinct rates of population of the $T_{+1}$, $T_0$, and $T_{-1}$ spin states and produces spin-polarized triplets. If doublet radical formation is fast enough to compete with the rate of spin-lattice relaxation ($T_1^{-1}$) of $^3MX^*$, the spin polarization is carried over to the doublet radicals with $T_{+1}$ and $T_{-1}$ triplets giving $\alpha$ and $\beta$ spin state doublet radicals, respectively. If the $T_{-1}$ level

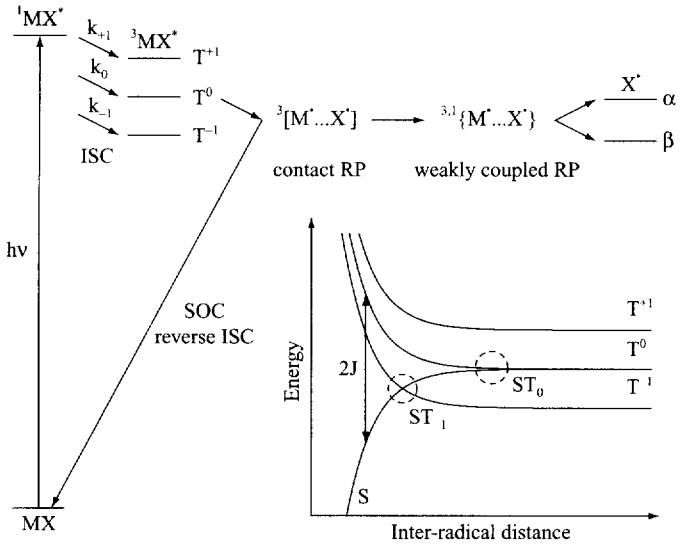


**Fig. 1.** Overview of the polarization development according to triplet (TM) and radical pair (RPM) CIDEP mechanisms in a bond cleavage reaction. The inset shows the energies of the singlet (S) and triplet ($T_{\pm1,0}$) states of a radical pair in a magnetic field as function of the inter-radical distance. The dashed circles mark the regions of efficient $ST_{-1}$ and $ST_0$ mixing.

has excess population, radical formation produces doublet radicals with spin polarization, $P = (N_\beta - N_\alpha)/(N_\beta + N_\alpha)$, larger than the polarization at thermal equilibrium ($P_B$). In that case the TREPR spectra will display enhanced absorption (A) signals. If the $T_{+1}$ level is preferentially populated, the free radicals carry negative spin polarization and spectra will be in emission (E). The mechanism is independent of nuclear spin state so that relative intensities of peaks given by hyperfine splittings are identical to those found at thermal equilibrium.

The fraction of the polarization with which the triplets are "born" that is ultimately captured by doublet radical products formed at a rate $k_f$ is given by $k_f T_1/(1 + k_f T_1)$. The triplet spin-lattice relaxation time ($T_1$) depends on the magnitudes of the zero-field splitting (zfs) parameters, the rotational correlation time $\tau_r$ and the Zeeman splitting [32]. Monomolecular reactions, such as the photoinduced bond homolysis reactions with which this review is concerned, can occur on a subnanosecond time scale so that $k_f > T_1^{-1}$. In that case, strong TM CIDEP can be generated [14]. However, it is important to note that the generation of spin polarization in triplet-state molecules requires that the lifetime of the triplets exceeds the inverse of the electron spin Larmor frequency, $\omega_0^{-1}$ [30]. Therefore, radical formation steps that occur on a femtosecond to low picosecond time scale will not give rise to TM CIDEP. Furthermore, in the case of transition-metal complexes, triplet excited states may have significant metal atomic orbital character. This will give rise to very short spin-lattice relaxation times [33] that may also preclude the generation of triplet spin polarization.



The relative population
try character of the excited
polarization can give inform
in the radical formation st
tetraphenylporphyrins (TPP
as donor, the TREPR spec
TM CIDEP [27, 34, 35]. W
tron donor, the TM signal
reflects the effect of meta
state of these porphyrins. T
ing the values of the zfs p
Values of these parameters
precursor triplets [37].

In most cases, photoexc
thermalized first excited si
occurs. Hence, TM CIDE
length. However, if ISC is
relaxation, TM CIDEP ma
length-dependent spin pola
radicals produced in photo
will be discussed further
diimine)] complex also ge
spin polarization attributed
The wavelength dependen
curs on a (sub)picosecond

Photochemical reactions t
radical pair (RP) intermed
duced by the singlet (S)-tr
(see Fig. 1, inset) [12, 13
mixing of the S and $T_0$ R
interaction $J$ between the u
RPM). $ST_0$ mixing is driv
two spins, $\Delta\omega$, and involv
contact radical pair is gen
the solvent cage so that $J$
the third, the radicals ree
expressed in the form of
spin for the other.

According to $ST_0$ RPM
ponent in the spectrum of
pair [M$^\cdot$···R$^\cdot$] is proportio

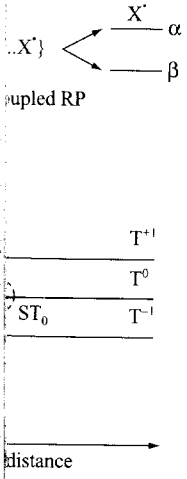





iplet (TM) and radical pair (RPM)
the energies of the singlet (S) and
n of the inter-radical distance. The
and $ST_0$ mixing.

ublet radicals with spin po-
olarization at thermal equi-
lisplay enhanced absorption
ited, the free radicals carry
ission (E). The mechanism
intensities of peaks given
at thermal equilibrium.
triplets are "born" that is
ed at a rate $k_f$ is given by
$(T_1)$ depends on the mag-
rotational correlation time
ctions, such as the photoin-
ew is concerned, can occur
nat case, strong TM CIDEP
note that the generation of
at the lifetime of the trip-
requency, $\omega_0^{-1}$ [30]. There-
ond to low picosecond time
in the case of transition-
ificant metal atomic orbital
relaxation times [33] that
rization.

The relative population rates of the triplet sublevels depend on the symmetry character of the excited states involved in the ISC process so that TM spin polarization can give information on the characteristics of the triplet state involved in the radical formation step. For instance, in studies of the photooxidation of tetraphenylporphyrins (TPP) by quinones it was found that with ZnTPP triplets as donor, the TREPR spectra of the quinone anion radicals exhibit absorptive TM CIDEP [27, 34, 35]. With photoexcited MgTPP [34] or $H_2$TPP [36] as electron donor, the TM signal contribution is emissive. The switch from A to E reflects the effect of metal ion binding on the character of the triplet excited state of these porphyrins. The magnitude of TM CIDEP can be estimated knowing the values of the zfs parameters, $D$ and $E$, as well as the relative ISC rates. Values of these parameters can be derived from rigid-matrix TREPR spectra of precursor triplets [37].

In most cases, photoexcitation of a molecule is followed by relaxation to the thermalized first excited singlet state from which ISC to the triplet excited state occurs. Hence, TM CIDEP generally will be independent of excitation wavelength. However, if ISC is fast compared to internal conversion and vibrational relaxation, TM CIDEP may depend on the wavelength of excitation. A wavelength-dependent spin polarization pattern was found in the FTEPR spectra of radicals produced in photoinduced reactions of xanthone with alcohols [38]. As will be discussed further on, photoinduced bond homolysis in a [Ru(alkyl)(α-diimine)] complex also generates radicals with excitation wavelength-dependent spin polarization attributed to radical formation via higher excited states [17]. The wavelength dependence serves as a diagnostic of photochemistry that occurs on a (sub)picosecond timescale.

### *3.2 Radical Pair Mechanism*

Photochemical reactions that lead to free radical formation normally generate radical pair (RP) intermediates. Radical pair mechanism (RPM) CIDEP is produced by the singlet (S)-triplet (T) spin state evolution of this transient species (see Fig. 1, inset) [12, 13, 28, 31, 39]. RPM spin polarization can be due to mixing of the S and $T_0$ RP states ($ST_0$ RPM) or, in the case that the exchange interaction $J$ between the unpaired electrons is less than 0, S and $T_{-1}$ states ($ST_{-1}$ RPM). $ST_0$ mixing is driven by the difference in precession frequencies of the two spins, $\Delta\omega$, and involves a three-step process [28, 31]. In the first step the contact radical pair is generated. In the second, the radicals diffuse apart within the solvent cage so that $J \sim \Delta\omega$ and $T_0 \leftrightarrow S$ interconversion can take place. In the third, the radicals reencounter and the effect of the spin-state evolution is expressed in the form of excess α electron spin for one radical and excess β spin for the other.

According to $ST_0$ RPM theory [3, 4], the intensity of the $i$th hyperfine component in the spectrum of the radical $R^\bullet$ generated by dissociation of the radical pair $[M^\bullet \cdots R^\bullet]$ is proportional to [40]

$$P_i = C_i(\Delta\omega_i^{1/2} - \gamma\Delta\omega_i). \quad (1)$$

Here $\Delta\omega_i$ represents half the difference in resonance frequencies of the two radicals and is determined by $\Delta g = (g_R - g_M)$ and hyperfine interactions. The magnitude of the polarization $P_i$ depends on the radical pair lifetime so that it is expected to increase with increasing solvent viscosity. In media in which radical pair dissociation is inhibited, i.e., high-viscosity solvents, or in systems for which the $ST_0$ mixing terms are large, $ST_0$ RPM spin polarization can be generated as well without the separation-reencounter scenario [39]. The contribution of this direct process is represented by the last term in Eq. (1). The weighing factor $\gamma$ in most cases is close to zero.

The sign of the proportionality constant $C_i$ in Eq. (1) depends on the position of the resonance peak, the sign of $J$, and the spin multiplicity of the excited state precursor from which the RP is formed. Assuming $J < 0$, as is the case normally, all resonance peaks from radical 1 positioned on the low-field side of the center of the spectrum from radical 2 will be in E and those on the high-field side will be in A if the precursor is an excited triplet. The reverse pattern, AE, will be found if the precursor is a singlet excited state. There is evidence that $J > 0$ in some radical ion pair reactions [41]. In that case the patterns are reversed.

$ST_0$ RPM CIDEP does not create net spin polarization but redistributes spins over the two radicals of the pair. If it is the single source of spin polarization, integration of the TREPR spectrum will yield zero overall signal intensity if the spectra of both radicals can be detected. This can serve as a diagnostic of spin polarization produced by $ST_0$ RPM CIDEP alone.

If hyperfine interactions are large, or the exchange and Zeeman interactions are of similar magnitude, $ST_{-1}$ ($J < 0$) or $ST_{+1}$ ($J > 0$) can be a source of RPM spin polarization [3]. In the case of radical formation via a triplet excited state and $ST_{-1}$ mixing by a positive hfcc ($A > 0$), the spectrum will be in emission with the low-field side enhanced relative to the high-field side. An absorption spectrum with a stronger polarization on the high-field side is generated if the precursor is in a singlet excited state and $A > 0$. If $A < 0$, the polarization will still be emissive for a triplet precursor and absorptive for a singlet precursor, but the enhancement of the hyperfine lines will be reversed (stronger on the high-field half or on the low-field half of the spectrum for triplet or singlet precursor, respectively).

The $ST_{-1}$ spin polarization contribution will increase in importance in viscous solutions in which slow diffusional motion increases the time during which the radical separation is such that S and $T_{-1}$ states are of the order of the hfccs (see Fig. 1, inset). The polarization contribution produced by the hyperfine couplings of radical 1 ($A_1$) is proportional to $A_1^2[I_1(I_1 + 1) - m_1(m_1 + 1)]$, where $I_1$ and $m_1$ denote the overall nuclear spin state quantum numbers. The polarization produced by $ST_{-1}$ mixing due to hyperfine couplings of radical 2 must be added to this term. The procedure of calculating the relative intensities of hyperfine components given by $ST_{-1}$ RPM CIDEP is described in the literature [3].



A number of features
polarization transfer genera
doublet radicals in absorpti
peaks are identical to those
RPM CIDEP no net polari
AE pattern and relative in
one radical depend strongl
trum of the other radical.
polarization, but the relati
those found at thermal equ
signal contribution is contr
precursor or the radical fo
molysis reactions considere
compared with the instrum
polarization, by contrast, is
formed. In the case of a s
RPM buildup can serve to
first-order radical formatio
ond timescale may be obs
RP spin state [42–44].

Spin-orbit coupling (SOC)
rise to a back reaction giv
tronic state (see Fig. 1).
ates spin polarization if th
can compete with spin-lat
in photochemically genera
cess has been found in T
thene dyes by quinones [4
halogen-substituted N,N-d
evident from the fact that
of the halogen substituent
reverse TM CIDEP is driv
atoms in the reactant, it
transition-metal complexes

## 4 Photoind

Reviews dealing with the
transition-metal complexes
the studies dealt with ma

A number of features distinguish TM from RPM CIDEP. First, TM spin polarization transfer generates net polarization and leaves the spectra of both doublet radicals in absorption or emission, while relative intensities of hyperfine peaks are identical to those found at Boltzmann equilibrium. By contrast, in $ST_0$ RPM CIDEP no net polarization is produced, the spectra will exhibit an EA or AE pattern and relative intensities of hyperfine components in the spectrum of one radical depend strongly on their position relative to the center of the spectrum of the other radical. The $ST_{-1}$ (or $ST_{+1}$) mechanism also produces net polarization, but the relative intensities of hyperfine components deviate from those found at thermal equilibrium [3]. Second, the rise time of the TM CIDEP signal contribution is controlled by the spin-lattice relaxation time of the triplet precursor or the radical formation rate if $k_f > T_1^{-1}$. In the case of the bond homolysis reactions considered in this review, the rise time is expected to be short compared with the instrument response time since $k_f^{-1}$, $T_1 < 10^{-8}$ s. RPM spin polarization, by contrast, is generated throughout the lifetime of the radical pairs formed. In the case of a second-order radical formation step, the time profile of RPM buildup can serve to determine the reaction rate [10, 11, 27, 34]. In fast first-order radical formation processes, RPM CIDEP development on a nanosecond timescale may be observable and would reflect the time evolution of the RP spin state [42–44].

### *3.3 Reverse TM CIDEP*

Spin-orbit coupling (SOC) in a triplet exciplex or triplet contact RP can give rise to a back reaction giving the original reactant molecule in the ground electronic state (see Fig. 1). This reverse ISC process is spin-selective and generates spin polarization if the rate of the dissociation of the surviving radical pair can compete with spin-lattice relaxation [45, 46]. Evidence for spin polarization in photochemically generated free radicals as a result of this reverse ISC process has been found in TREPR studies of oxidative quenching of triplet xanthene dyes by quinones [47] and reductive quenching of triplet duroquinone by halogen-substituted N,N-dimethylanilines [48, 49]. The role played by SOC is evident from the fact that net spin polarization grows in as the atomic number of the halogen substituent on the xanthene and aniline molecules increases. Since reverse TM CIDEP is driven by SOC arising because of the presence of "heavy" atoms in the reactant, it can play a role in photochemical reactions involving transition-metal complexes.

## 4 Photoinduced Homolysis of Metal-Alkyl Bonds

Reviews dealing with the spin selectivity of photochemical reactions involving transition-metal complexes have been published previously [33, 50]. In most cases the studies dealt with magnetic field effects on reaction kinetics and reaction

yields measured with the aid of optical spectroscopy. The number of applications of TREPR in this field of research remains limited because of the difficulty to detect the transient paramagnetic species formed. TREPR techniques have been used successfully, however, in studies of the mechanisms of alkyl radical formation by photoinduced bond homolysis of metal-alkyl complexes.

An early example is the application of cw TREPR in the study of methyl radical formation by photoinduced homolysis of the Co-$CH_3$ bond in a bis(dimethylglyoximato)cobalt complex (methylcobaloxime, $[(CH_3)(H_2O)Co(dmg)_2]$) [14]. The four-line spectrum due to the $CH_3^{\bullet}$ radical formed by photolysis of this complex in water and 2-propanol was found to be in emission with relative line intensities close to the binomial 1:3:3:1 ratio. This was taken as evidence that the Co-$CH_3$ bond cleavage reaction proceeds via the triplet excited state of the cobaloxime (TM CIDEP). Another application of cw TREPR concerned the study of the photodissociation of bis(*S*-benzyl-1,2-diphenyl-1,2-ethylenedithiolato)Me, where Me is Ni, Pd, or Pt [51, 52]. Photoexcitation of these complexes leads to the elimination of both benzyl groups. The goal of the study was to find out if the reaction occurs in two steps or if both benzyl groups are split off in a concerted reaction. In the case of the Ni and Pd complexes, the spectra displayed a multiline spectrum centered at $g = 2.0021$ assigned to the benzyl radical and a broad resonance peak at $g = 2.042$ (Ni) or $g = 2.014$ (Pd). The broad peak was attributed to the paramagnetic metal complex produced by the removal of one benzyl group and it was concluded that the benzyl groups split off in consecutive steps. The intermediate paramagnetic metal complexes were found to lose the remaining benzyl group in a dark reaction occurring on a time scale of 10 to 20 min. With the Pt complex only the benzyl radical spectrum was detected. All spectra were in absorption, but showed some intensity asymmetry that could point to an EA RPM contribution. The dominant absorptive signal contribution was ascribed to TM CIDEP and it was concluded that the bond cleavage reaction involves the triplet excited state of the complexes.

### *4.1 Bond Cleavage Reactions in $B_{12}$ Coenzymes and Model Compounds*

#### 4.1.1 [(R)Cobalamin], R = Methyl or Adenosyl

Enzymatic reactions involving cobalamins (I) (Fig. 2a), vitamin $B_{12}$ coenzymes, have been shown to involve a transient radical pair intermediate and reaction kinetics in part may be controlled by the spin state evolution in this transient [53]. This has led to a number of investigations dealing with the mechanism of photoinduced bond cleavage in cobalamins. Recent femtosecond to nanosecond transient optical absorption studies of the Co-$CH_3$ bond homolysis of I-Me in aqueous solution show a strong wavelength dependence of the reaction mechanism [54–57]. Excitation at 520–530 nm results within 40 ps in the formation of a transient (100% yield) with about 1 ns lifetime and the characteristics of an ion-pair state $\{CH_3^- Co^+\}$. Excitation with 400 nm light, on the other hand,



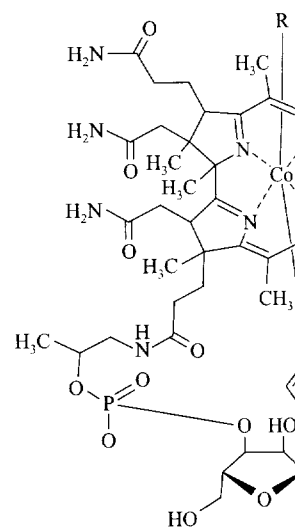

R-cobalam

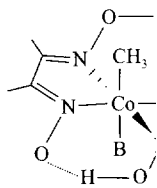

B = $H_2O$ or Py

Methylcobalc

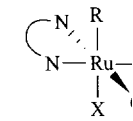

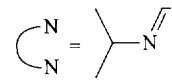

R = methyl, iso-pro

X = I or $SnPh_3$

**Fig. 2.** Structural formulas of **a**

results in 25% direct bon
and 75% creation of the
tion wavelength, the long
the geminate radical pair

py. The number of applica-
imited because of the diffi-
ned. TREPR techniques have
mechanisms of alkyl radical
l-alkyl complexes.
PR in the study of methyl
Co-$CH_3$ bond in a bis(di-
ne, $[(CH_3)(H_2O)Co(dmg)_2]$)
formed by photolysis of this
emission with relative line
was taken as evidence that
triplet excited state of the
TREPR concerned the study
l-1,2-ethylenedithiolato)Me,
of these complexes leads to
he study was to find out if
oups are split off in a con-
xes, the spectra displayed a
o the benzyl radical and a
(Pd). The broad peak was
ed by the removal of one
roups split off in consecu-
plexes were found to lose
ring on a time scale of 10
cal spectrum was detected.
nsity asymmetry that could
sorptive signal contribution
at the bond cleavage reac-
es.

*and Model Compounds*

Adenosyl

), vitamin $B_{12}$ coenzymes,
intermediate and reaction
evolution in this transient
ng with the mechanism of
emtosecond to nanosecond
ond homolysis of I-Me in
ce of the reaction mecha-
in 40 ps in the formation
and the characteristics of
light, on the other hand,

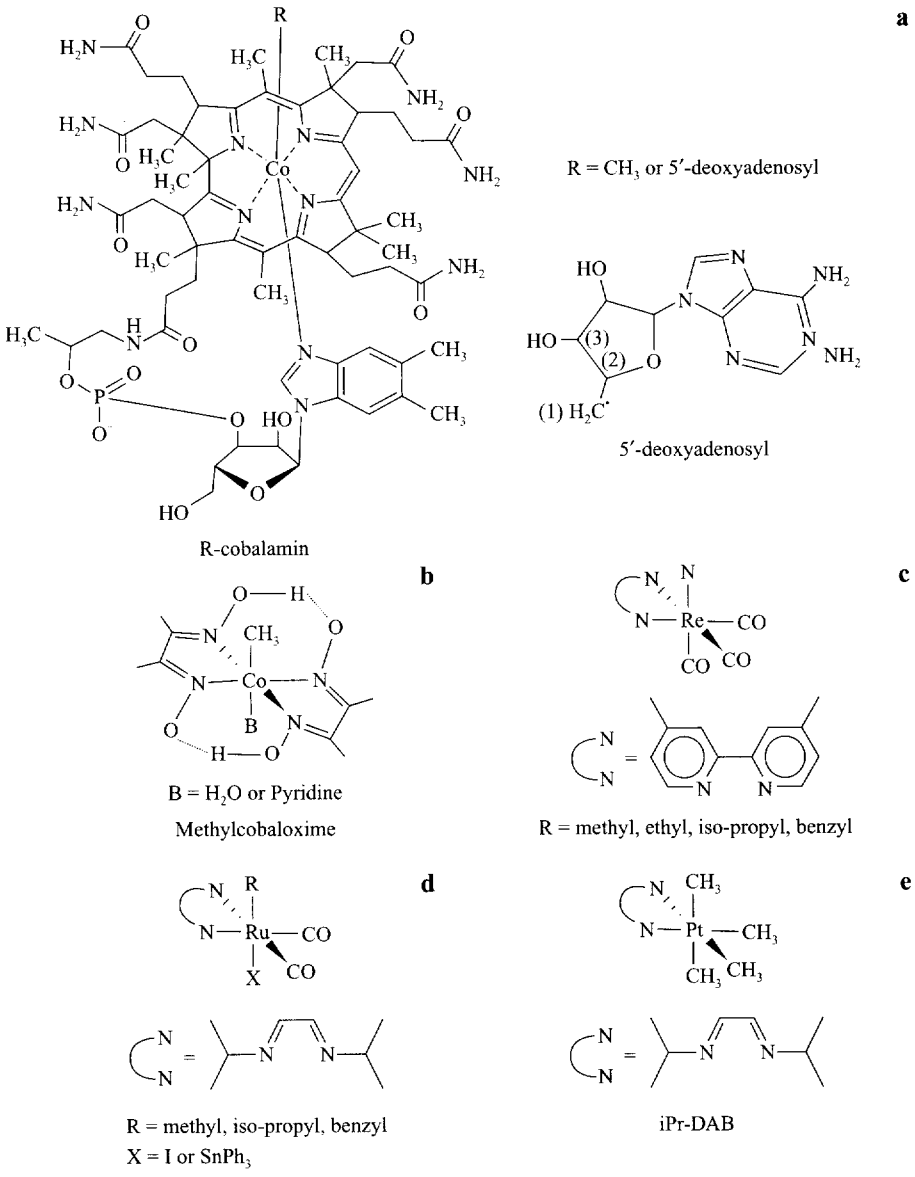


**Fig. 2.** Structural formulas of **a** cobalamins, **b** methylcobaloxime, **c** $Re(R)(CO)_3(dmb)$, **d** $Ru(X)(R)(CO)_2(iPr\text{-}DAB)$, **e** $Pt(CH_3)_4(iPr\text{-}DAB)$.

results in 25% direct bond homolysis giving the geminate radical pair $[CH_3^{\bullet}\cdots Co^{\bullet}]$ and 75% creation of the ion-pair species $\{CH_3^- Co^+\}$. Regardless of the excitation wavelength, the long-lived intermediate undergoes bond homolysis to form the geminate radical pair $[CH_3^{\bullet}\cdots Co^{\bullet}]$ in 14% yield, while 86% reverts back to I-

Me. The wavelength effect establishes the existence of two distinct routes of formation of [Co•···$CH_3^•$] radical pairs; one dominates when exciting in the first absorption band of the complex and the other when exciting in the second absorption band. In the case of I-Ad in aqueous solution, no wavelength dependence was found [55]. Transient optical absorption spectra indicate that bond homolysis occurs exclusively via the direct route [56].

The optical studies do not give direct information on the spin state of the precursors of the radical pair, although it has been assumed that bond cleavage involves singlet excited states [55] and magnetic field effects on reaction yield also point to a reactive singlet excited state [53]. Direct information on the spin multiplicity of the excited state could be provided by TREPR measurements on the organic free radicals formed and this has prompted an FTEPR study of bond homolysis in I-Me and I-Ad [15]. Of particular interest was the question whether or not the wavelength dependence affects CIDEP effects and if this provides additional mechanistic insights. Results of this work are summarized below.

Figure 3 displays the FTEPR spectra given by I-Me in aqueous solution at 11°C upon excitation with 355 and 532 nm laser light for a delay time of 80 ns. The spectrum corresponds to that of the $CH_3^•$ radical ($A_H$ = 2.26 mT, $g$ = 2.0025 [58]). No EPR signal from the Co(II) complex formed was observed. This complex is expected to give rise to a broad-line spectrum due to incomplete averaging of $g$ and hyperfine anisotropies positioned on the low-field side of the $CH_3^•$ spectrum ($g_{Co} \sim 2.2$–$2.3$ [59–61]). Figure 3 shows that with 532 nm excitation, the intensity pattern deviates slightly from the thermal equilibrium 1:3:3:1 pattern with the high-field half of the spectrum enhanced relative to the low-field half and that this asymmetry becomes slightly more pronounced when the excitation wavelength is shifted to 355 nm. The time profile of the $CH_3^•$ signal intensity (not shown) displays an initial fast decay (about 200 ns) followed by a slower decay on the microsecond time scale. The fast decay time constant matches the spin-lattice relaxation time of methyl radicals in aqueous solutions [62] confirming that signal intensity at early time is determined by CIDEP. Subsequent slower signal decay reflects the kinetics of radical scavenging reactions. Figure 3 also presents spectra given by I-Me in 1,2-propanediol. In this case the intensity pattern shows no significant excitation wavelength dependence and is similar to that given by I-Me in aqueous solution on excitation at 355 nm.

The nuclear spin-dependent CIDEP must be due to the spin-state development in a precursor radical pair (RPM CIDEP, cf. Sect. 3.2). Furthermore, the excitation wavelength-dependent spin polarization found for I-Me in aqueous solution establishes unequivocally that there must be competing reaction channels. Apparently, bond cleavage can occur fast enough to compete with processes that produce the relaxed first singlet (or triplet) excited state of the complex. It can be concluded that the data given by I-Me in aqueous solution are fully consistent with the wavelength dependence found in flash photolysis studies [55].

Figure 4 displays the FTEPR spectra given by adenosylcobalamin (I-Ad) in aqueous solution at 10°C upon laser excitation at 355 or 532 nm (delay time,




I-Me in

**Fig. 3.** FTEPR spectra of the m
(bottom) of methylcobalamin (I
perature. I

80 ns). The spectrum is
($A_{H1}(2)$ = 2.21 mT) and t
mT). The simulated spec
with the spectrum expect
the spectrum of this radi
sorption peaks with the
In contrast with the $CH_3^•$
pattern is independent o
also showed no wavelen

of two distinct routes of for-
when exciting in the first
n exciting in the second ab-
ution, no wavelength depen-
spectra indicate that bond
66].
ion on the spin state of the
assumed that bond cleavage
eld effects on reaction yield
rect information on the spin
y TREPR measurements on
ed an FTEPR study of bond
st was the question whether
effects and if this provides
are summarized below.
-Me in aqueous solution at
ght for a delay time of 80
adical ($A_H$ = 2.26 mT, $g$ =
formed was observed. This
pectrum due to incomplete
on the low-field side of the
ws that with 532 nm excita-
thermal equilibrium 1:3:3:1
anced relative to the low-
more pronounced when the
e profile of the $CH_3^\bullet$ signal
about 200 ns) followed by
e fast decay time constant
dicals in aqueous solutions
letermined by CIDEP. Sub-
adical scavenging reactions.
ropanediol. In this case the
elength dependence and is
excitation at 355 nm.
to the spin-state develop-
ect. 3.2). Furthermore, the
ound for I-Me in aqueous
competing reaction chan-
ugh to compete with pro-
) excited state of the com-
Me in aqueous solution are
d in flash photolysis stud-

lenosylcobalamin (I-Ad) in
5 or 532 nm (delay time,

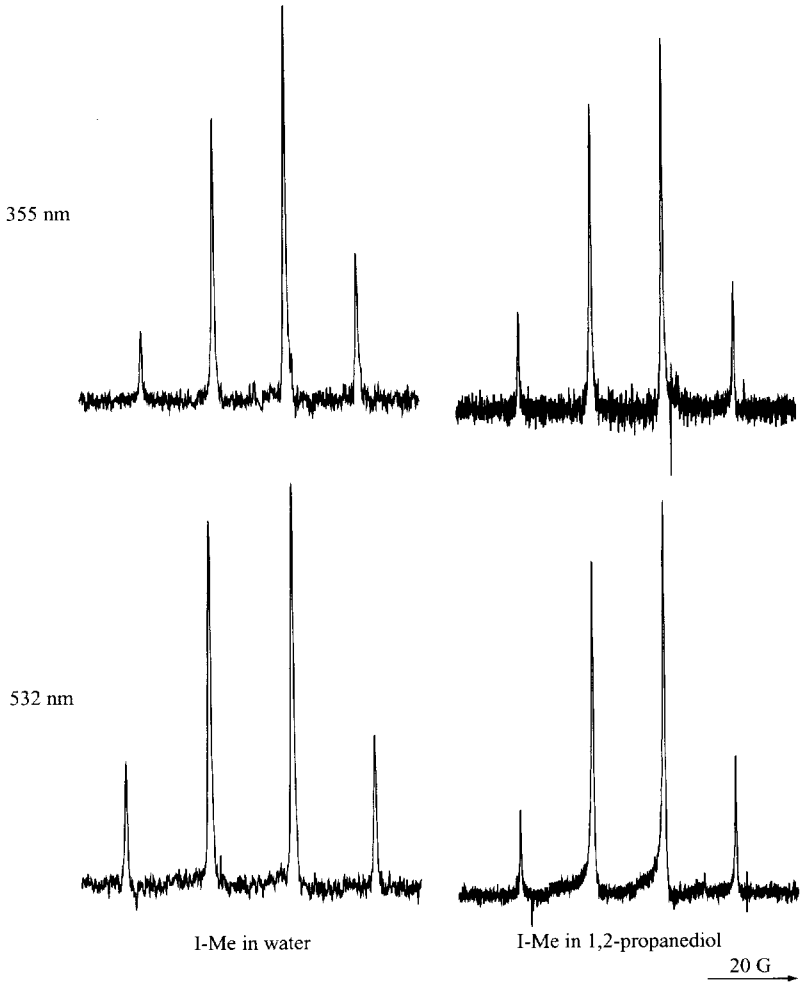


**Fig. 3.** FTEPR spectra of the methyl radical produced upon laser excitation at 355 (top) and 532 nm (bottom) of methylcobalamin (I-Me, $\sim 10^{-3}$ M) in water at 11°C and 1,2-propanediol at room temperature. Delay time of 80 ns, absorption peaks point up.

80 ns). The spectrum is centered at $g$ = 2.0097 and shows a triplet splitting ($A_{H1}(2)$ = 2.21 mT) and two doublet splittings ($A_{H2}(1)$ = 0.161 mT, $A_{H3}(1)$ = 0.059 mT). The simulated spectrum is shown at the bottom of Fig. 4. It is consistent with the spectrum expected for the 5′-deoxyadenosyl radical. To our knowledge, the spectrum of this radical has not been reported before. The spectra show absorption peaks with the high-field side enhanced relative to the low-field side. In contrast with the $CH_3^\bullet$ spectra given by I-Me in aqueous solution, the CIDEP pattern is independent of excitation wavelength. Flash photolysis measurements also showed no wavelength dependence for this system [55].

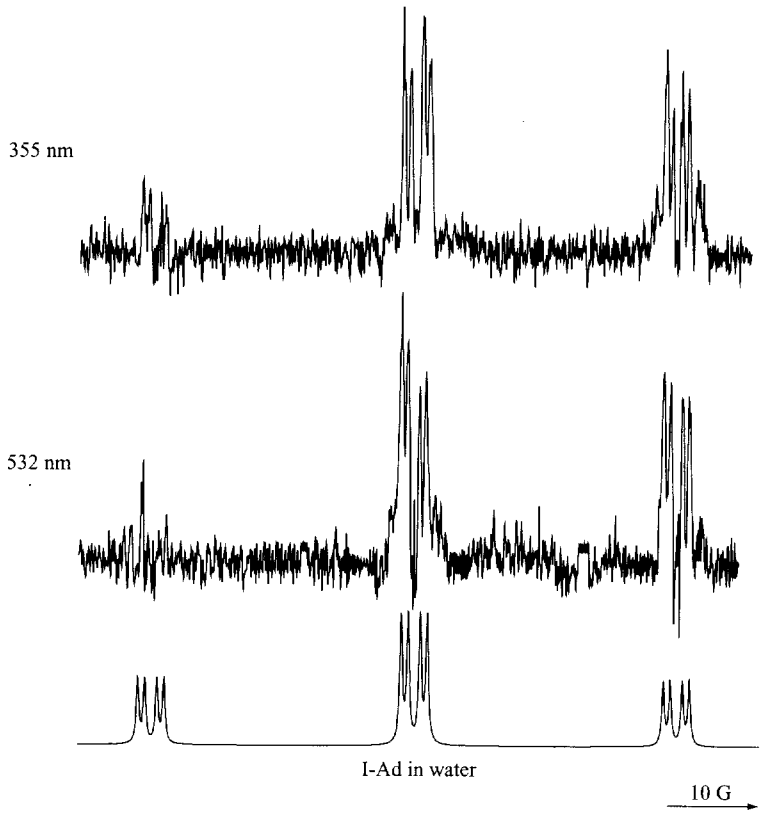


**Fig. 4.** FTEPR spectra of the adenosyl radical produced upon laser excitation at 355 (top) and 532 nm (middle) of aqueous solutions of adenosylcobalamine (I-Ad, $\sim 10^{-3}$ M, 10°C). Delay time of 80 ns, absorption peaks point up. The simulated spectrum (bottom) is based on the hfcc's given in the text.

The question of the CIDEP mechanism(s) responsible for the observed intensity patterns at this time cannot be answered with certainty. The observation of nuclear spin-dependent CIDEP (cf. Figs. 3 and 4) establishes that RPM CIDEP plays a role [3, 4]. Originally it was proposed that the spectral features can be accounted for by assuming radical pair formation via a singlet excited state reaction where spin polarization is generated by the $ST_{-1}$ RPM [15]. However, this interpretation failed to take into account that the sign of the proton hfcc in the methyl radical is expected to be negative [7]. According to the rules summarized in Sect. 3.2, the $ST_{-1}$ mechanism would give rise to an absorption spectrum if the radical pair is formed via a singlet excited state of the cobalamin. However, with $A_{CH_3} < 0$ the intensity of the low-field side of the spectrum should be enhanced relative to the high-field side contrary to what is observed. Spin polarization generated by $ST_0$ mixing in a radical pair can account, at least semi-quantitatively, for the intensity patterns since $g_{Co} > g_{CH_3}$ [59]. However, this would imply a triplet excited state bond homolysis route (assuming that $J < 0$, see Sect.



3.2) and conflicts with ea
excited state [53, 55]. Sinc
spin polarization and radi
path – for instance, via a
the nuclear spin-dependen

It is noteworthy that t
tively small effect on the
the strong effect on the re
to flash photolysis measur
from $H_2O$ (viscosity $\eta =$
($\eta = 40.4$ cP, $\varepsilon = 27.5$) (c
RPM CIDEP is strongly
with parallel reaction route
ger effects have been fou
tion channel generates si
dominant contribution to
Since flash photolysis m
tively long-lived intermed
wavelength, whereas pron
near UV [55], this interp
intensity is derived predo
if the prompt path is a
escape "instantaneously"
allowed, back reaction.
through RP S ↔ T mixin

4.1.2 [(C

The photoinduced homoly
$Co(dmg)_2$] (II) (Fig. 2b),
63, 64]. The interest in t
larity to the cobalamins
standing of the mechanis
zymes. Since the synthes
straightforward [65], they
of structure–reactivity re

As noted previously,
tochemistry of transition-m
$H_2O$) complex [14]. Phot
propanol generates $CH_3^{\bullet}$
spectrum with an intensit
The observed spin polar
evidence that bond homo
[14]. An alternative inte

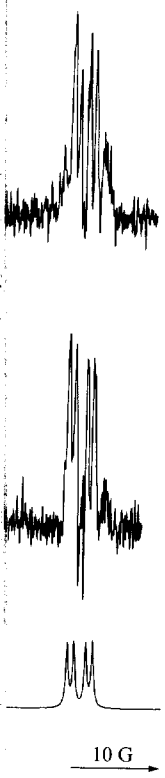


tion at 355 (top) and 532 nm
10°C). Delay time of 80 ns,
the hfcc's given in the text.

e for the observed in-
tainty. The observation
ishes that RPM CIDEP
pectral features can be
inglet excited state re-
PM [15]. However, this
the proton hfcc in the
g to the rules summa-
to an absorption spec-
tate of the cobalamin.
of the spectrum should
what is observed. Spin
account, at least semi-
]. However, this would
g that $J < 0$, see Sect.

3.2) and conflicts with earlier conclusions that bond cleavage involves a singlet excited state [53, 55]. Since signal intensity in TREPR spectra is the product of spin polarization and radical concentration, it is possible that a minor reaction path – for instance, via a triplet excited state in this case – is responsible for the nuclear spin-dependent intensity pattern.

It is noteworthy that the variation in excitation wavelength has only a relatively small effect on the FTEPR spectra given by I-Me (cf. Fig. 3) considering the strong effect on the relative importance of the two reaction routes according to flash photolysis measurements [55]. Similarly, the effect of the solvent change from $H_2O$ (viscosity $\eta = 1.0$ cP, dielectric constant $\varepsilon = 78.5$) to 1,2-propanediol ($\eta = 40.4$ cP, $\varepsilon = 27.5$) (cf. Fig. 3) is remarkably small in view of the fact that RPM CIDEP is strongly dependent on solvent properties [3, 4]. In other cases with parallel reaction routes and/or two or more CIDEP contributions, much stronger effects have been found (see below). The results suggest that only one reaction channel generates significant spin polarization and, therefore, makes the dominant contribution to the FTEPR signal independent of reaction conditions. Since flash photolysis measurements show that radical formation via the relatively long-lived intermediate $\{CH_3^- \; Co^+\}$ takes place independent of excitation wavelength, whereas prompt bond homolysis occurs only upon excitation in the near UV [55], this interpretation leads to the conclusion that the FTEPR signal intensity is derived predominantly from the former path. It can be speculated that if the prompt path is a singlet excited state reaction route, only radicals that escape "instantaneously" into the bulk of the solution avoid the efficient, spin-allowed, back reaction. This may not leave time to generate spin polarization through RP S ↔ T mixing processes.

### 4.1.2 $[(CH_3)(B)Co(dmg)_2]$, B = $H_2O$ or Pyridine

The photoinduced homolytic cleavage of the Co-R bond in cobaloximes, $[(R)(B)\times Co(dmg)_2]$ (II) (Fig. 2b), has been a subject of a number of EPR studies [14, 63, 64]. The interest in these compounds stems in part from the structural similarity to the cobalamins (I). It suggests that their study could aid in the understanding of the mechanism of enzymatic reactions involving vitamin $B_{12}$ coenzymes. Since the synthesis of cobaloximes with a variety of R and B groups is straightforward [65], they are convenient model compounds for detailed studies of structure–reactivity relationships.

As noted previously, an early application of TREPR in the study of the photochemistry of transition-metal complexes concerned the $[(CH_3)(H_2O)Co(dmg)_2]$ (II-$H_2O$) complex [14]. Photoexcitation of solutions of this complex in water or 2-propanol generates $CH_3^\bullet$ radicals that give rise to an emissive four-line TREPR spectrum with an intensity pattern that closely matches the binomial distribution. The observed spin polarization was attributed to TM CIDEP and was taken as evidence that bond homolysis occurs via a triplet excited state of the complex [14]. An alternative interpretation of the data cannot be excluded, however. As

the authors note, the $ST_0$ RPM is expected to give a CIDEP pattern that shows only minor deviations from the binomial distribution.

Relative intensities given by $ST_0$ mixing can be estimated by the fact that the spin polarization for the *i*th hyperfine component in the spectrum of the $CH_3^{\bullet}$ radical is approximately proportional to the square root of its frequency offset from the center of the resonance due to the Co(II) complex (Eq. (1), Sect. 3.2). With $g_{CH_3} = 2.0025$, $A_{CH_3} = 2.26$ mT [58], and $g_{Co} \sim 2.25$ [60], the calculated relative intensities from low field to high field are 0.94:2.91:3:1.03. The calculation neglects to take into account the hfccs of the Co(II) complex. In addition, the values of the *g*-factor and hfcc's of this complex are very sensitive to solvent changes [60]. The actual intensity ratio, therefore, will deviate somewhat from the one given here. Even so, the calculation indicates that the $ST_0$ RPM intensities can match the binomial intensity ratio within measurement accuracy. The observed emissive spectrum, therefore, can be due to a singlet excited state reaction path in which the $ST_0$ RPM is responsible for the spin polarization.

Recently, FTEPR has been used to investigate the effects of cobaloxime structure, solvent medium, and temperature on spin polarization. The objective of this study was to get more definitive information on the mechanism of photoinduced bond homolysis through observed CIDEP effects. Of particular interest was the question whether or not the mechanism of photolysis is similar to that of the cobalamins. Some preliminary results of this work have been published [15]. Here a more complete account of the outcome of the investigation is presented. Experimental details will be published elsewhere (C. Kiarie et al., unpubl.).

Figure 5 displays the room temperature FTEPR spectra obtained upon photoexcitation (355 nm; delay time, 50 ns) of $10^{-3}$ M solutions of $[(CH_3)(H_2O)Co(dmg)_2]$ (II-$H_2O$) and $[(CH_3)(Py)Co(dmg)_2]$ (II-Py) in solvents with similar viscosities but increasing dielectric constants. The four-line spectra are due to the $CH_3^{\bullet}$ radical [58]. As in the case of the cobalamins, no signal from the Co(II) counter radical was observed due to a short $T_2$ which causes the signal to decay within the spectrometer deadtime. In aqueous solution both complexes give rise to E polarized spectra with intensity patterns close to 1:3:3:1 in agreement with the result reported by Sakaguchi et al. [14]. However, the polarization is found to exhibit a remarkably strong solvent dependence, changing from E to A on going from water to toluene. Notwithstanding this dramatic effect, the intensity pattern remains very close to symmetric irrespective of solvent.

Figure 5 show that low-polarity solvents (i.e., toluene) give A polarized spectra, whereas polar solvents give E polarized spectra. In the case of II-Py, the change tracks the change in solvent dielectric constant. Results obtained with II-$H_2O$ indicate that specific solute–solvent interactions, such as the coordination ability of the solvent molecule, as well as the identity of the axially ligated base plays an important role. In the case of this complex, the polarization patterns observed with toluene and $H_2O$ as solvents are similar to those given by II-Py in these solvents. However, with ethanol and pyridine the polarization patterns given by II-$H_2O$ are the reverse of those generated by II-Py. The "anomaly" very likely reflects the difference in the ability of pyridine and ethanol to coordinate



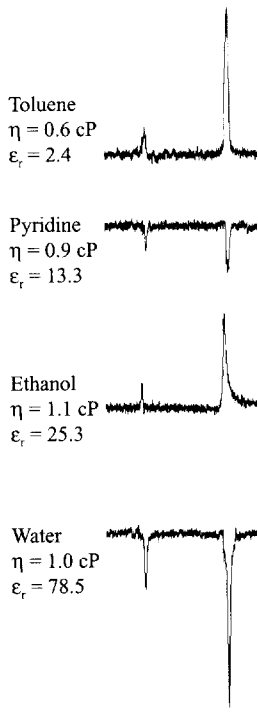


**Fig. 5.** Room temperature FTEI
nm) of about $10^{-3}$ M solutions
low-viscosity solvents with incr
viscosities $\eta$ and relative diele

to the transition-metal ion
could play an important r
be significant if SOC-ind
spin polarization.

CIDEP effects also a
ture. Figure 6 (left) displa
nm, 50 ns) of the II-$H_2O$
constants but strongly di
cosity causes a switch ir
to E (1,2-propanediol, $\eta$
the FTEPR spectra given
6, right). In the latter ca
tion pattern becomes evid
($\eta = 1.1$ cP) is in absor

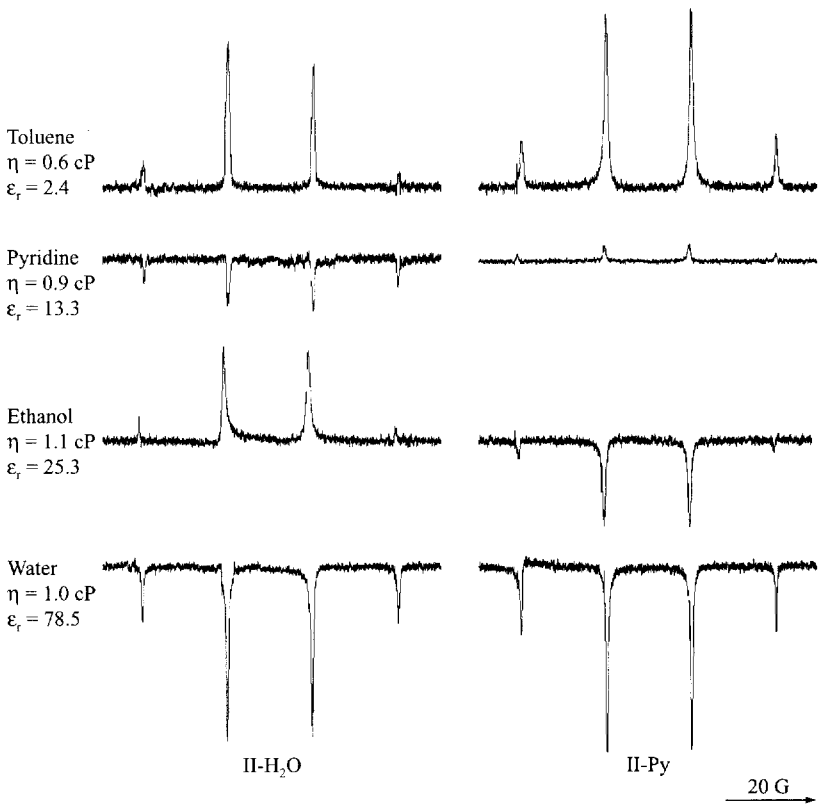


**Fig. 5.** Room temperature FTEPR spectra from the methyl radical produced by photoexcitation (355 nm) of about $10^{-3}$ M solutions of $[(CH_3)(H_2O)Co(dmg)_2]$ (II-$H_2O$) and $[(CH_3)(Py)Co(dmg)_2]$ (II-Py) in low-viscosity solvents with increasing dielectric constants for a delay time setting of 50 ns. Solvent viscosities $\eta$ and relative dielectric constants $\varepsilon_r$ are given in the figure. Absorption peaks point up.

to the transition-metal ion in the axial position vacated by the methyl group. This could play an important role in the development of RPM CIDEP and also could be significant if SOC-induced reverse ISC [45, 46] (cf. Sect. 3.3) contributes to spin polarization.

CIDEP effects also are found to depend on solvent viscosity and temperature. Figure 6 (left) displays the signals of $CH_3^{\bullet}$ generated by photoexcitation (355 nm, 50 ns) of the II-$H_2O$ complex in a series of alcohols with similar dielectric constants but strongly differing viscosities. It is found that an increase in viscosity causes a switch in polarization from A (methanol, $\eta = 0.5$ cP, $\varepsilon = 32.6$) to E (1,2-propanediol, $\eta = 40.4$ cP, $\varepsilon = 27.5$). A similar effect is observed in the FTEPR spectra given by II-$H_2O$ in ethanol as the temperature is reduced (Fig. 6, right). In the latter case, a pronounced nuclear-spin-state-dependent polarization pattern becomes evident as the temperature is reduced. The spectrum at 12°C ($\eta = 1.1$ cP) is in absorption with the low-field half enhanced relative to the

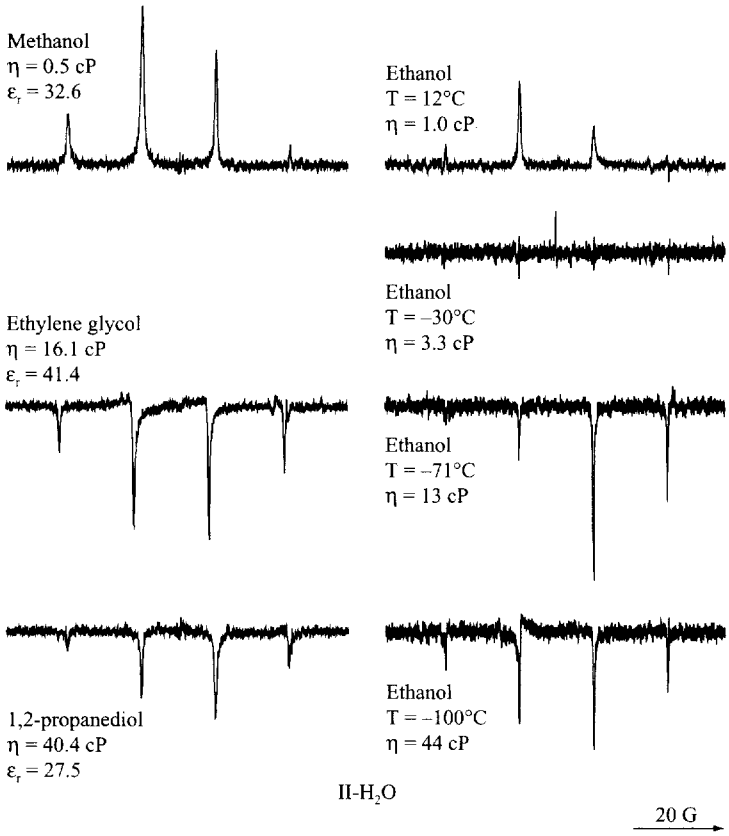


**Fig. 6.** FTEPR spectra from the methyl radical produced upon photoexcitation (355 nm) of solutions of $[(CH_3)(H_2O)Co(dmg)_2]$ (II-$H_2O$, about $10^{-3}$ M) in solvents with increasing viscosities at room temperature and in ethanol at reduced temperatures. Delay time of 50 ns. Solvent viscosities $\eta$ and temperatures are given in the figure. Absorption peaks point up.

high-field half. The intensity of this spectrum is considerably less than that of the spectrum obtained at room temperature. At −30°C (3.3 cP) the lines are barely visible. At −71 (13 cP) and −100°C (46 cP) the spectra have the resonance lines in emission with the high-field half enhanced compared with the low-field half. A gradual change from A to E was found as well for II-Py in pyridine as the temperature was lowered (not shown).

As noted above, the $ST_0$ RPM is not expected to give rise to a pronounced nuclear-spin-state-dependent polarization pattern. The same is the case for the $ST_{-1}$ mechanism. In this case spin polarization is proportional to $A^2[I(I+1) - m(m+1)]$ and is made up of contributions from the proton hfcc of the $CH_3^{\bullet}$ radical and the hfcc's of the Co(II) complex (Sect. 3.2) [3, 4]. The latter make the dominant contribution to the mixing of the $S \leftrightarrow T_{-1}$ radical pair states so that relative intensities of the $CH_3^{\bullet}$ resonance peaks should be close to those found



at thermal equilibrium. Inc
($I_{Co}$ = 7/2, $A_{Co}$ ~ 5.4 mT
sity pattern is 0.94:2.95:3
polarization is found in s
ture and in ethanol at low
assuming that the observe
CIDEP contributions, one
of net A and E polarizat
component. For instance,
may have a dominant A
tensity pattern. As the ten
grow in because of the i
two contributions then ca
relative to high-field lines
an E spectrum with high-
−71°C). Cancellation of
tion in overall signal stre
from II-$H_2O$ in ethanol.

The transition from A
ity) solvent medium (cf.
CIDEP mechanisms. The
associated with competing
lar to those found for the
tion from an A to an E s
the reaction paths. Confi
tolysis measurements sim
would also be of interest
tation wavelength for the
sorption band only).

*4.2 Metal-Al*

Kleverlaan et al. [16, 18
study the photoinduced n
diimine)] (III), [Ru(L)(R)
plexes (Fig. 2c–e). R is
or I, and α-diimine is 4
1,4-diazabutadiene (iPr-D
spectra recorded on irrad
band belongs to an elec
transfer (MLCT) in chara
level on model complex
transition has mainly ML

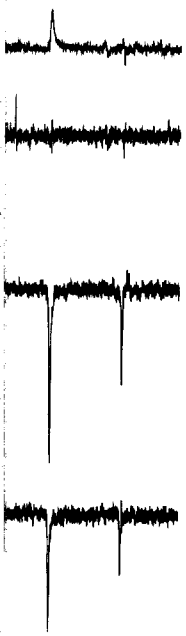

20 G

:citation (355 nm) of solutions
easing viscosities at room tem-
Solvent viscosities $\eta$ and tem-
s point up.

erably less than that of
(3.3 cP) the lines are
e spectra have the reso-
compared with the low-
well for II-Py in pyri-

ve rise to a pronounced
ame is the case for the
ortional to $A^2[I(I + 1) -$
on hfcc of the $CH_3^{\bullet}$ radi-
4]. The latter make the
dical pair states so that
e close to those found

at thermal equilibrium. Including only the effects of the $CH_3^{\bullet}$ proton and Co hfcc's ($I_{Co} = 7/2$, $A_{Co} \sim 5.4$ mT [60]) in the calculation, the approximate $ST_{-1}$ intensity pattern is 0.94:2.95:3:0.98. Nevertheless, a pronounced hyperfine-dependent polarization is found in spectra given by II-$H_2O$ in methanol at room temperature and in ethanol at low temperatures (Fig. 6). This can only be explained by assuming that the observed intensity patterns are the sum of opposing (A + E) CIDEP contributions, one stemming from the RPM, where (partial) cancellation of net A and E polarization contributions enhances the nuclear-spin-dependent component. For instance, the spectrum at room temperature and low viscosity may have a dominant A TM CIDEP contribution giving the binomial 1:3:3:1 intensity pattern. As the temperature is reduced, an E $ST_0$ RPM contribution could grow in because of the increased lifetime of the radical pair. The sum of the two contributions then can give an A spectrum with low-field lines enhanced relative to high-field lines (Fig. 6, 12°C) or, as RPM CIDEP becomes dominant, an E spectrum with high-field lines enhanced relative to low-field lines (Fig. 6, −71°C). Cancellation of opposing CIDEP contributions would lead to a reduction in overall signal strength and this is exactly what is observed in the spectra from II-$H_2O$ in ethanol.

The transition from A to E upon an increase in polarity of the (low-viscosity) solvent medium (cf. Fig. 5) can be accounted for as well in terms of two CIDEP mechanisms. The solvent effect suggests that the two mechanisms are associated with competing channels of photoinduced Co-$CH_3$ bond cleavage similar to those found for the structurally similar methylcobalamin [55]. The transition from an A to an E spectrum then signifies a shift in relative importance of the reaction paths. Confirmation of this interpretation would require flash photolysis measurements similar to those carried out on the cobalamins [54–57]. It would also be of interest to perform FTEPR measurements as function of excitation wavelength for the cobaloximes (so far excitation was in the second absorption band only).

### *4.2 Metal-Alkyl Bond Cleavage Reactions in α-Diimine Transition Metal Complexes*

Kleverlaan et al. [16, 18, 19] and van Slageren et al. [17, 20] used FTEPR to study the photoinduced metal-alkyl bond cleavage in a series of [Re(R)$(CO)_3$(α-diimine)] (III), [Ru(L)(R)$(CO)_2$(α-diimine)] (IV) and Pt(R)$_4$(α-diimine) (V) complexes (Fig. 2c–e). R is alkyl (methyl, ethyl, isopropyl or benzyl), L is $SnPh_3$ or I, and α-diimine is 4,4′-dimethyl-2,2′-bipyridine (dmb) or *N*,*N*′-diisopropyl-1,4-diazabutadiene (iPr-DAB). In the case of complexes III, resonance Raman spectra recorded on irradiation into the lowest absorption band showed that this band belongs to an electronic transition that is mainly metal-to-ligand charge transfer (MLCT) in character [66]. Molecular orbital calculations at the CASSCF level on model complexes suggested that the allowed lowest-energy electronic transition has mainly MLCT character with a small admixture of sigma-bond-to-

ligand charge transfer (SBLCT) character [67]. However, these complexes have a low-lying $^3$SBLCT state, which is higher (R = Me) or lower (R = Et, iPr, Bz) in energy than the lowest $^3$MLCT state. Population of these SBLCT states from the $^{1,3}$MLCT states leads to Re-R bond homolysis [19, 66, 68, 69] in the case of R = Et, iPr and Bz. When R = Me, radical formation occurs on a femtosecond time-scale, in competition with the decay to the lowest $^3$MLCT state which is presumed to be nonreactive. The lowest electronic transition of complexes IV (L = I) has halide-to-ligand charge transfer character [70]. Once more, for L = I and R = iPr, Bz, crossing occurs to reactive $^3$SBLCT states, leading to Ru-R bond homolysis [16, 71]. For complexes IV (L = $SnPh_3$) and V, the lowest $^1$SBLCT state is directly optically accessible. This was proven by resonance Raman studies [72, 73] as well as MO calculations [67, 72].

For a few of these compounds the light-induced formation of free radicals could be demonstrated with conventional EPR measurements either by direct detection of the paramagnetic species at low temperature or with the aid of the spin-trapping method [19, 66]. Conventional EPR measurements on related complexes, including metal-metal bonded compounds, were also reported [68, 74, 75]. With FTEPR the transient alkyl (or benzyl) radicals formed upon pulsed-laser excitation of the complexes in fluid solution at room temperature could be monitored directly with nanosecond time resolution. The FTEPR studies illustrated the remarkably strong effects that solvent dielectric constant and viscosity can have on CIDEP generated in photoinduced metal-alkyl bond cleavage reactions [16–20]. Also, one system was found to exhibit strong wavelength-dependent CIDEP [18]. This provides unequivocal evidence that bond cleavage occurs with a rate that competes with internal conversion processes following excitation in higher excited states of the complex. In the following, salient results of the FTEPR studies concerned with these complexes will be reviewed. The focus primarily will be on metal-$CH_3$ bond homolysis reactions, complete accounts of the investigations can be found in the literature [16–20].

### 4.2.1 [Re(R)(CO)$_3$(dmb)] and [Ru(I)(R)(CO)$_2$(iPr-DAB)]

FTEPR spectra from the methyl radicals produced by photoexcitation (355 nm) of solutions of [Re($CH_3$)(CO)$_3$(dmb)] (III-$CH_3$) and [Re($CD_3$)(CO)$_3$(dmb)] (III-$CD_3$) in toluene at room temperature for $\tau_d$ settings of 50 ns and 1 μs are presented in Fig. 7 [19]. The signal rise time is instrument controlled, in agreement with results of time-resolved optical absorption studies which show that bond homolysis occurs within the time span of the laser pulse [19]. No FTEPR signal from the [Re(CO)$_3$(dmb)]$^\bullet$ counter radical was observed. However, it was possible to detect this radical with cw EPR in frozen 2-propanol at 133 K and in toluene at room temperature [19]. The [Re(CO)$_3$(dmb)]$^\bullet$ radical gives rise to a broad (ca. 30 G) resonance with a $g$-value (2.005–2.008) slightly above that of the methyl radical (ca. 2.002). That the $g$-value of the [Re(CO)$_3$(dmb)]$^\bullet$ radical is close to the free electron value leads to the conclusion that the orbital of




**Fig. 7.** FTEPR spectra from the
M solutions of [Re($CH_3$)(CO)$_3$(
and **d**) in toluene at room temp

the unpaired electron in t
the unpaired electron resi

The spectrum of the
Fig. 7a), displays EA pol
pattern). The intensity pa
cursor triplet radical pair
(cf. Sect. 3.2). The effec
assignment. Figure 7b sh
larization almost complet
According to Eq. (1), the
of the difference in reson
pair. The strong depende
action shows that the va
nificantly on the differen
nating contributions from
result of cw EPR measure
and $CH_3^\bullet$ are very similar

lowever, these complexes have
Me) or lower (R = Et, iPr, Bz)
n of these SBLCT states from
s [19, 66, 68, 69] in the case
nation occurs on a femtosecond
lowest $^3$MLCT state which is
ic transition of complexes IV
ter [70]. Once more, for L = I
T states, leading to Ru-R bond
$_3$) and V, the lowest $^1$SBLCT
ven by resonance Raman stud-

ced formation of free radicals
neasurements either by direct
erature or with the aid of the
measurements on related com-
were also reported [68, 74, 75].
cals formed upon pulsed-laser
m temperature could be moni-
FTEPR studies illustrated the
nstant and viscosity can have
bond cleavage reactions [16–
wavelength-dependent CIDEP
d cleavage occurs with a rate
following excitation in higher
salient results of the FTEPR
eviewed. The focus primarily
mplete accounts of the inves-

)(CO)$_2$(iPr-DAB)]

by photoexcitation (355 nm)
d [Re(CD$_3$)(CO)$_3$(dmb)] (III-
s of 50 ns and 1 μs are pre-
trument controlled, in agree-
ion studies which show that
laser pulse [19]. No FTEPR
as observed. However, it was
zen 2-propanol at 133 K and
$_3$(dmb)]$^\bullet$ radical gives rise to
)5–2.008) slightly above that
of the [Re(CO)$_3$(dmb)]$^\bullet$ radi-
conclusion that the orbital of

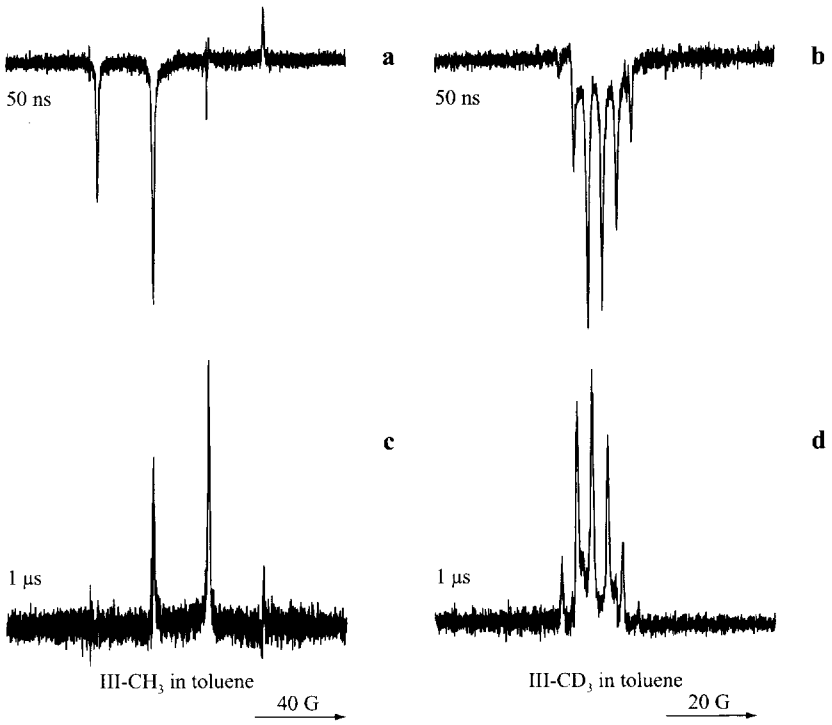


**Fig. 7.** FTEPR spectra from the methyl radical produced by photoexcitation (355 nm) of about $2 \cdot 10^{-3}$ M solutions of [Re(CH$_3$)(CO)$_3$(DMB)] (III-CH$_3$) (**a** and **c**) and [Re(CD$_3$)(CO)$_3$(DMB)] (III-CD$_3$) (**b** and **d**) in toluene at room temperature. Delay times of 50 ns (**a** and **b**) and 1 μs (**c** and **d**), absorption peaks point up.

the unpaired electron in this complex has very little metal ion character and that the unpaired electron resides in a diimine $\pi^*$ orbital.

The spectrum of the $CH_3^\bullet$ radical obtained at short delay times ($\tau_d$ = 50 ns, Fig. 7a), displays EA polarization with net overall emission (denoted as an E*A pattern). The intensity pattern points to a polarization contribution from a precursor triplet radical pair, $^3$[Re(CO)$_3$(dmb)$^\bullet\cdots$CH$_3^\bullet$], generating ST$_0$ RPM CIDEP (cf. Sect. 3.2). The effect of deuteration on the observed CIDEP confirms this assignment. Figure 7b shows that the isotopic substitution removes the EA polarization almost completely so that the spectrum of $CD_3^\bullet$ is entirely in emission. According to Eq. (1), the magnitude of the ST$_0$ RPM contribution is a function of the difference in resonance frequency ($\Delta\omega$) of the two radicals that form the pair. The strong dependence of CIDEP on the magnitude of the hyperfine interaction shows that the values of $\Delta\omega$ in the case of III-CH$_3$ do not depend significantly on the difference in $g$-values of the two radicals but contains dominating contributions from the $CH_3^\bullet$ hyperfine splitting. This is consistent with the result of cw EPR measurements which show that the $g$-values of [Re(CO)$_3$(dmb)]$^\bullet$ and $CH_3^\bullet$ are very similar in magnitude [19]. Deuteration reduces the hyperfine

splitting by about a factor of six and the resulting reduction in $\Delta\omega$ produces the pronounced reduction in EA signal contribution.

Evidence that signal intensities are determined primarily by CIDEP effects is provided by the observation that the time evolution of the spectra during the first microsecond is controlled by spin-lattice relaxation. Spectra recorded at longer delay times (Fig. 7c, d) display absorption signals given by thermally equilibrated methyl radicals. From the time profiles of signal intensities (not shown) it was determined that spin-lattice relaxation times in toluene at room temperature are $89\pm24$ and $103\pm20$ ns for $CH_3^{\bullet}$ and $CD_3^{\bullet}$, respectively.

In addition to the EA RPM $ST_0$ CIDEP contribution, there is a CIDEP mechanism that produces net emission and that makes the dominant contribution to the $CD_3^{\bullet}$ spectrum shown in Fig. 7b. This CIDEP component could be due to TM CIDEP which would be consistent with the proposal that bond dissociation involves a triplet excited state of III-$CH_3$ [19]. However, the assignment of one of the CIDEP components to the TM does not agree with conclusions reached in an ultrafast time-resolved electronic absorption study [76]. According to this study, ISC to a nonreactive $^3$MLCT state and a reactive $^3$SBLCT state can occur from an optically populated nonrelaxed $^1$MLCT Franck-Condon state. The $^3$SBLCT state produces radicals in less than 400 fs, a time scale too short for the TM to be operative (cf. Sect. 3.1, [3]). The conclusion that the $^3$MLCT state is unreactive was reached because measurements with TRIR and transient absorption spectroscopy showed that decay of this state was not accompanied by a noticeable increase in the radical concentration. The net E signal contribution could signify that the $^3$MLCT state is not completely unproductive. In this respect it is important to note that if the spin polarization created by TM CIDEP is high, only a small quantum yield is necessary to produce a measurable contribution in the EPR spectrum. An alternative explanation is that the $^3$SBLCT state produces a tightly coupled radical pair in which the reverse ISC process discussed in Sect. 3.3 [45, 46] produces the observed spin polarization component.

FTEPR spectra (not shown) given by the ethyl radical (Et$^{\bullet}$, hfcc's of 2.68 and 2.20 mT) produced by photolysis (355 nm) of [Re(Et)$(CO)_3$(dmb)] (III-Et) in toluene or 2-propanol are completely in emission with no significant RPM CIDEP contribution [16]. By contrast, spectra of the isopropyl radicals (iPr$^{\bullet}$, hfcc's of 2.46 and 2.16 mT) produced by pulsed-laser excitation (355 nm) of [Re(iPr)$(CO)_3$(dmb)] (III-iPr) in 2-propanol and toluene are completely in absorption [18]. The CIDEP patterns are not affected by a change in excitation wavelength (355, 532 nm). Spin polarization for both complexes is attributed to TM CIDEP. The change from an E spectrum to an A spectrum on going from III-Et to III-iPr illustrates the extreme sensitivity of CIDEP to minor changes in the excited state character of the complex. The spectrum given by III-iPr in 2-propanol shows a slight asymmetry with the high-field side enhanced relative to the low-field side that is attributed to an additional EA $ST_0$ RPM contribution. The magnitude of the spin polarization created by RPM CIDEP is a strong function of radical pair lifetime and increases with increasing solvent viscosity. This ac-



counts for the increase in
panol. Initial signal decays
reflect relaxation to therma
time profiles are $0.23\pm0.5$
μs) for iPr$^{\bullet}$ in toluene (2-

FTEPR spectra (not sl
0.18 and 0.62 mT) prod
[Re(Bz)$(CO)_3$(dmb)] (III-B
in this case the spectrum
metry with enhanced high-
the CIDEP pattern change
polarization is made up o
and an EA $ST_0$ RPM CI
RPM, as expected, increas
increases in solvent visco
pair lifetime. From the tim
values of $T_1$ of $9.1\pm0.6$
reported for Bz$^{\bullet}$ in propa

In summary, CIDEP o
[Re(R)$(CO)_3$(dmb)] compl
agreement with conclusion
ies. Both TM and $ST_0$ RP
nism, as expected, increas
lifetime is increased. The
Bz) spin polarization cont
excited state character of
possible that the switch i
TM to a T → S reverse I

Results obtained with
are very similar to those
the spectra are in absorpt
an E*A polarization patte
trum in toluene (2-propa
obtained. As in the case
of the spin polarization p
bond cleavage reaction g
a combination of TM an

4.2.2 [Ru$(CH_3)$(S

Photoinduced methyl rad
$(CO)_2$(iPr-DAB)] (IV-CH
detailed FTEPR study can
the FTEPR spectra of the

reduction in $\Delta\omega$ produces the

l primarily by CIDEP effects
tion of the spectra during the
laxation. Spectra recorded at
n signals given by thermally
les of signal intensities (not
ion times in toluene at room
nd $CD_3^{\bullet}$, respectively.
tion, there is a CIDEP mecha-
dominant contribution to the
nponent could be due to TM
sal that bond dissociation in-
wever, the assignment of one
ree with conclusions reached
study [76]. According to this
active $^3$SBLCT state can oc-
T Franck-Condon state. The
s, a time scale too short for
nclusion that the $^3$MLCT state
with TRIR and transient ab-
ate was not accompanied by
The net E signal contribution
ely unproductive. In this re-
zation created by TM CIDEP
o produce a measurable con-
lanation is that the $^3$SBLCT
nich the reverse ISC process
ved spin polarization compo-

l radical (Et$^{\bullet}$, hfcc's of 2.68
[Re(Et)(CO)$_3$(dmb)] (III-Et)
on with no significant RPM
the isopropyl radicals (iPr$^{\bullet}$,
laser excitation (355 nm) of
ene are completely in absorp-
a change in excitation wave-
omplexes is attributed to TM
ectrum on going from III-Et
EP to minor changes in the
m given by III-iPr in 2-pro-
side enhanced relative to the
$ST_0$ RPM contribution. The
CIDEP is a strong function
g solvent viscosity. This ac-

counts for the increase in the EA contribution on going from toluene to 2-propanol. Initial signal decays could be fit satisfactorily with single exponentials and reflect relaxation to thermal equilibrium. $T_1$ values derived from signal intensity time profiles are $0.23\pm0.5$ μs ($0.26\pm0.5$ μs) for Et$^{\bullet}$ and $1.0\pm0.5$ μs ($1.2\pm0.5$ μs) for iPr$^{\bullet}$ in toluene (2-propanol) [16].

FTEPR spectra (not shown) of the benzyl radical (Bz$^{\bullet}$, hfcc's, 1.63, 0.52, 0.18 and 0.62 mT) produced by photoexcitation (355 nm) of solutions of [Re(Bz)(CO)$_3$(dmb)] (III-Bz) display a net A polarization feature [16]. However, in this case the spectrum given by III-Bz in toluene shows a pronounced asymmetry with enhanced high-field side and upon a switch in solvent to 2-propanol, the CIDEP pattern changes to EA$^{\bullet}$. As in the case of the III-iPr complex, spin polarization is made up of an A signal contribution, attributed to TM CIDEP, and an EA $ST_0$ RPM CIDEP contribution. The contribution made by the $ST_0$ RPM, as expected, increases with increase in radical size (iPr$^{\bullet}$ versus Bz$^{\bullet}$) and increases in solvent viscosity because of the accompanying increase in radical pair lifetime. From the time evolution of the Bz$^{\bullet}$ spectrum in toluene (2-propanol) values of $T_1$ of $9.1\pm0.6$ μs ($12.7\pm0.7$ μs) were obtained. A $T_1$ of 15 μs was reported for Bz$^{\bullet}$ in propanediol at room temperature [77].

In summary, CIDEP observed in the spectra given by radicals given by the [Re(R)(CO)$_3$(dmb)] complexes suggest a triplet excited state reaction path in agreement with conclusions reached in earlier spectroscopic and theoretical studies. Both TM and $ST_0$ RPM CIDEP contributions are evident. The latter mechanism, as expected, increases in importance under conditions where radical pair lifetime is increased. The TM can make an E (III-$CH_3$, III-Et) or A (III-iPr, III-Bz) spin polarization contribution. This may reflect the effect of changes in the excited state character of the complex on the ISC process. Alternatively, it is possible that the switch in spin polarization signifies a change from a S → T TM to a T → S reverse ISC process (Sect. 3.3).

Results obtained with [Ru(I)(R)(CO)$_2$(iPr-DAB)] (IV, R = iPr, Bz) [16, 18] are very similar to those given by [Re(R)(CO)$_3$(dmb)] (R = iPr, Bz). In toluene the spectra are in absorption with high-field side enhanced, while in 2-propanol an E$^{\bullet}$A polarization pattern is found. From the time evolution of the iPr$^{\bullet}$ spectrum in toluene (2-propanol), values of $T_1$ of $1.2\pm0.5$ μs ($1.5\pm0.5$ μs) were obtained. As in the case of [Re(R)(CO)$_3$(dmb)], the strong solvent dependence of the spin polarization pattern is interpreted in terms of a triplet excited state bond cleavage reaction giving free radicals with spin polarization generated by a combination of TM and $ST_0$ RPM CIDEP.

### 4.2.2 [Ru($CH_3$)($SnPh_3$)(CO)$_2$(iPr-DAB)] and [Pt($CH_3$)$_4$(iPr-DAB)]

Photoinduced methyl radical formation from the complexes [Ru($CH_3$)($SnPh_3$)×(CO)$_2$(iPr-DAB)] (IV-$CH_3$) and [Pt($CH_3$)$_4$(iPr-DAB)] (V) was the subject of a detailed FTEPR study carried out by van Slageren et al. [17, 20]. Figure 8 depicts the FTEPR spectra of the $CH_3^{\bullet}$ and $CD_3^{\bullet}$ radicals produced by excitation of toluene

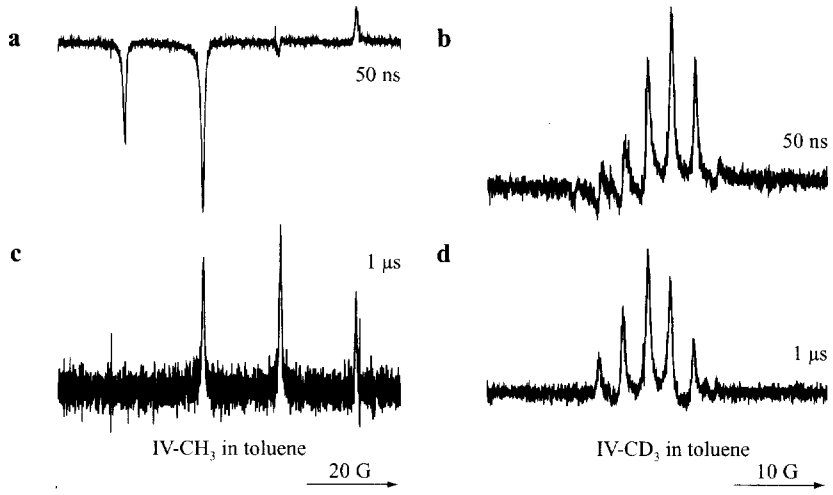


**Fig. 8.** FTEPR spectra from the methyl radical produced upon photoexcitation (355 nm) of about $2 \cdot 10^{-3}$ M solutions of $[Ru(SnPh_3)(CH_3)(CO)_2(iPr\text{-}DAB)]$ (IV-$CH_3$) (**a** and **c**) and $[[Ru(SnPh_3)(CD_3)(CO)_2(iPr\text{-}DAB)]$ (IV-$CD_3$) (**b** and **d**) in toluene at room temperature. Delay times of 50 ns (**a** and **c**) and 1 μs (**b** and **d**), absorption peaks point up.

solutions of IV-$CH_3$ and IV-$CD_3$ in the longest-wavelength absorption band of the complexes (excitation wavelength, 532 nm). For $\tau_d = 50$ ns, the spectrum of $CH_3^{\bullet}$ displays an E*A pattern very similar to the pattern observed in the spectrum given by $[Re(CH_3)(CO)_3(dmb)]$ (cf. Fig. 7a). Even so, CIDEP contributions must be different because deuteration has a totally different effect on the spectra given by the two complexes. As illustrated in Fig. 8b, $CD_3^{\bullet}$ generated by photolysis of IV-$CD_3$ in toluene gives a spectrum with a dominant net absorption component, whereas the spectrum of $CD_3^{\bullet}$ derived from $[Re(CD_3)(CO)_3(dmb)]$ (cf. Fig. 7b) is completely in emission. Moreover, the short-delay-time absorption spectrum given by IV-$CD_3$ in toluene (Fig. 8b) has an intensity that is very similar to that of the spectrum recorded 1 μs after the laser pulse. From this it can be concluded that the $CD_3^{\bullet}$ radicals are born with little or no spin polarization. Apparently there is no significant TM CIDEP contribution in this system. The absence of TM spin polarization is in agreement with experimental evidence that suggests that bond homolysis occurs extremely fast in these systems. For instance, the quantum yield is temperature independent and a function of excitation wavelength [75]. This indicates that the photoinduced bond homolysis reaction is an activationless process that occurs in competition with internal conversion and vibrational relaxation. As pointed out in Sect. 3.1, if the rate of radical formation from a triplet state precursor is fast compared to the electron spin Larmor frequency, spin-selective ISC does not give rise to TM CIDEP [30].

To explore the question of the CIDEP mechanisms that operate in the case of the IV-$CH_3$ and V complexes, solvent effects on the polarization patterns were examined. The results are presented in Figs. 9 and 10 [17]. Figure 9 shows that



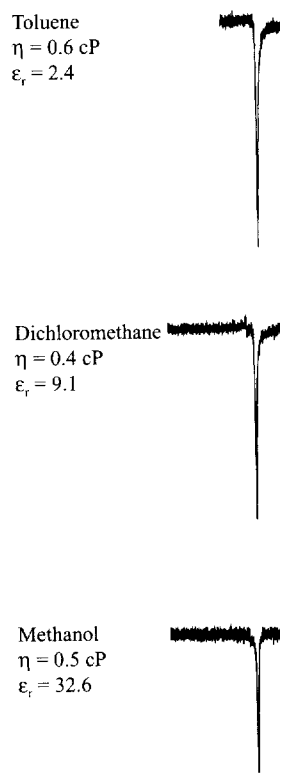


**Fig. 9.** Room temperature FTE
nm) of about $2 \cdot 10^{-3}$ M solutio
DAB)] (V) in solvents of incre
up. Viscosities

an increase in solvent po
($\varepsilon_r = 9.08$) to methanol
constant, leads to an inc
tensities appear to be un
trast, Fig. 10 shows that i
on the polarization patter
limited solubility of IV-C
ratio. In the case of $CD_3^{\bullet}$

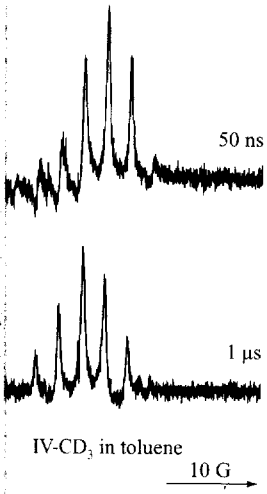


toexcitation (355 nm) of about $2 \cdot 10^{-3}$ d **c**) and [[Ru(SnPh$_3$)(CD$_3$)(CO)$_2$(iPr- y times of 50 ns (**a** and **c**) and 1 μs t up.

elength absorption band of the = 50 ns, the spectrum of $CH_3^{\bullet}$ rn observed in the spectrum so, CIDEP contributions must fferent effect on the spectra . 8b, $CD_3^{\bullet}$ generated by pho- h a dominant net absorption om [Re(CD$_3$)(CO)$_3$(dmb)] (cf. ort-delay-time absorption spec- ntensity that is very similar to ulse. From this it can be con- no spin polarization. Appar- a in this system. The absence mental evidence that suggests stems. For instance, the quan- of excitation wavelength [75]. s reaction is an activationless version and vibrational relax- dical formation from a triplet Larmor frequency, spin-selec-

ns that operate in the case of ne polarization patterns were 10 [17]. Figure 9 shows that

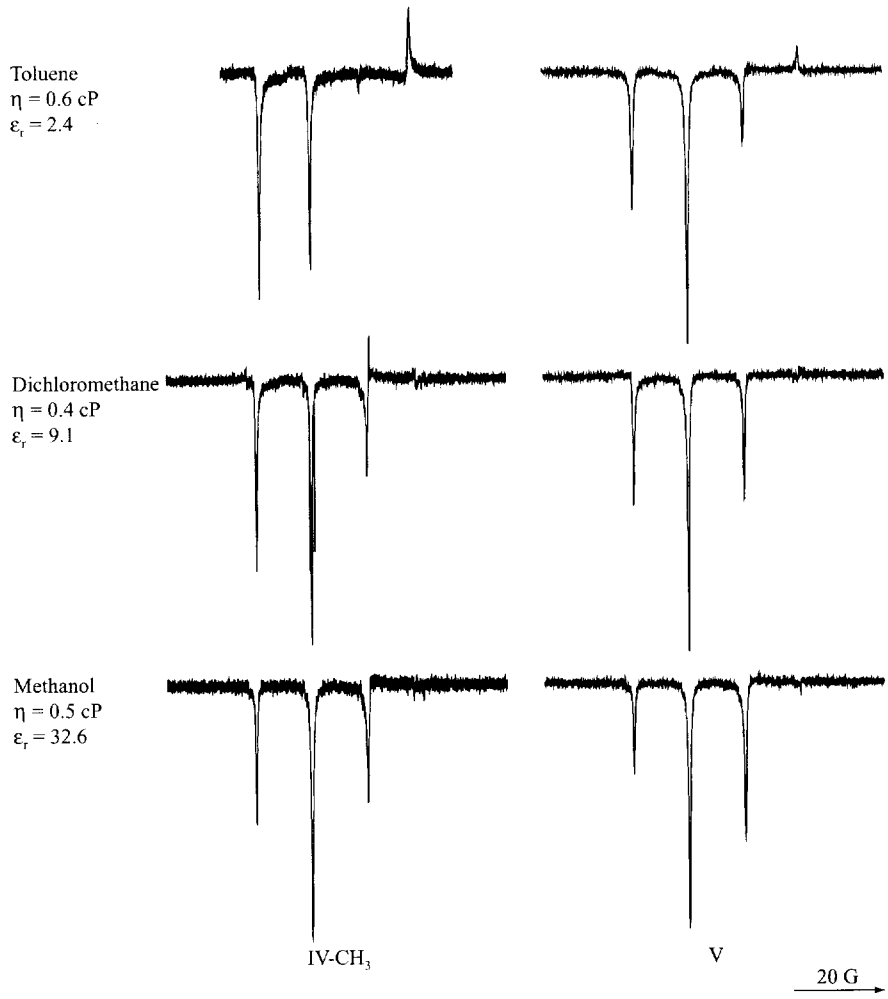


**Fig. 9.** Room temperature FTEPR spectra of the methyl radical produced by photoexcitation (532 nm) of about $2 \cdot 10^{-3}$ M solutions of [Ru(SnPh$_3$)(CH$_3$)(CO)$_2$(iPr-DAB)] (IV-CH$_3$) and [Pt(CH$_3$)$_4$(iPr-DAB)] (V) in solvents of increasing dielectric constant. Delay time of 50 ns, absorption peaks point up. Viscosities $\eta$ and dielectric constants $\varepsilon_r$ are given in the figure.

an increase in solvent polarity going from toluene ($\varepsilon_r = 2.38$) to dichloromethane ($\varepsilon_r = 9.08$) to methanol ($\varepsilon_r = 32.63$), while keeping the viscosity more or less constant, leads to an increase in the net emission signal contribution. Signal intensities appear to be unaffected by the changes in dielectric constant. By contrast, Fig. 10 shows that increases in viscosity of polar solvents have a minor effect on the polarization pattern but lead to a significant increase in signal intensity. The limited solubility of IV-CH$_3$ in ethylene glycol leads to a reduced signal-to-noise ratio. In the case of $CD_3^{\bullet}$ generated from IV-CD$_3$ (spectra not shown), the viscos-

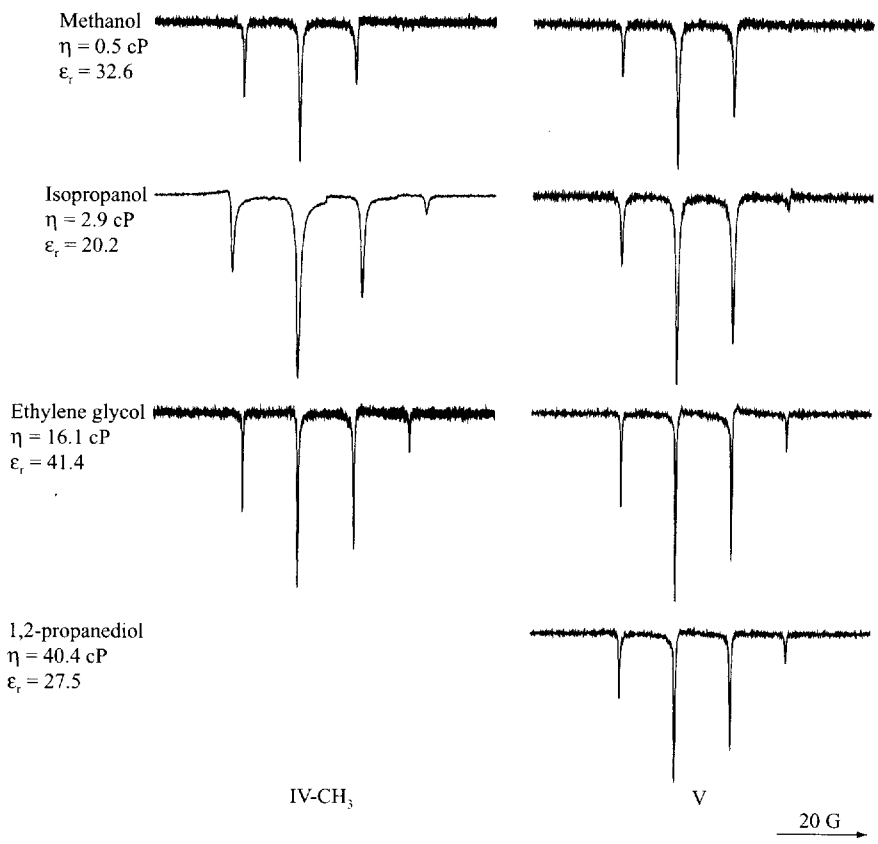


**Fig. 10.** Room temperature FTEPR spectra of the methyl radical produced by photoexcitation (532 nm) of about $2 \cdot 10^{-3}$ M solutions of $[Ru(SnPh_3)(CH_3)(CO)_2(iPr\text{-}DAB)]$ (IV-$CH_3$) and $[Pt(CH_3)_4(iPr\text{-}DAB)]$ (V) in solvents of increasing viscosity. Delay time of 50 ns, absorption peaks point up. Viscosity $\eta$ and relative dielectric constant $\varepsilon_r$ data are given in the figure.

ity effect on signal intensity is absent, which establishes that it must be due to an increase in polarization produced by a hyperfine-dependent CIDEP mechanism.

The CIDEP patterns of the spectra presented in Figs. 9 and 10 apparently are made up of an EA component and a net E component. In the case of IV-$CH_3$, both contributions are strongly reduced by deuteration of the methyl group (Fig. 8b) and, therefore, both must have their origin in RPM CIDEP. The EA contribution points to radical formation via a triplet excited state giving rise to an $ST_0$ RPM signal contribution. The net E contribution is consistent with $ST_{-1}$ RPM CIDEP [3, 4]. In the case of radical pair formation via a triplet excited state with $A_{CH_3} < 0$, this mechanism gives rise to an emissive signal contribution with the high-field lines enhanced relative to the low-field lines (cf. Sect. 3.2). An increase in solvent polarity apparently causes a slight change in the relative weights of the two RPM signal contributions (Fig. 9). This can be caused



by a solvent effect on th
generated by the RPM wi
Hence, the strong increas
viscosity (Fig. 10) is con
the two RPM mechanism

As shown in Fig. 11,
and $CD_3^{\bullet}$ formed by photo
strong excitation wavelen
energy absorption band ($\lambda$
pattern, while an EA* pa
($\lambda_{ex}$ = 308 and 355 nm).

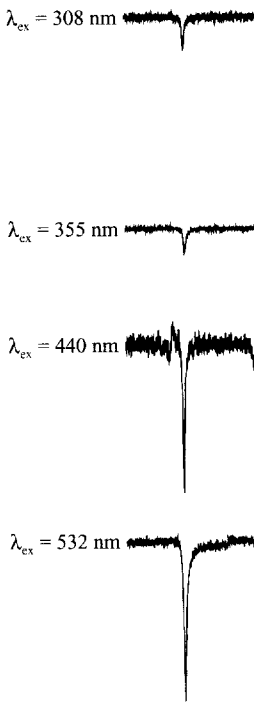


**Fig. 11.** Excitation wavelengt
by photoexcitation of about 2
and $[Ru(SnPh_3)(CD_3)(CO)_2(iPr\text{-}$
ns, absorption peaks

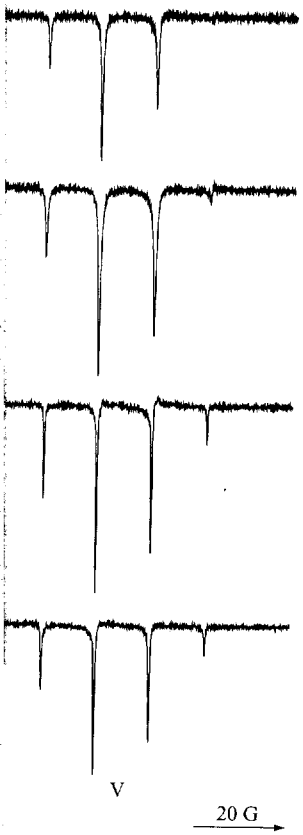


produced by photoexcitation (532
AB)] (IV-$CH_3$) and [$Pt(CH_3)_4$(iPr-
is, absorption peaks point up. Vis-
given in the figure.

es that it must be due to an
ndent CIDEP mechanism.
Figs. 9 and 10 apparently
ponent. In the case of IV-
eration of the methyl group
in RPM CIDEP. The EA
excited state giving rise to
ion is consistent with $ST_{-1}$
nation via a triplet excited
emissive signal contribu-
e low-field lines (cf. Sect.
ses a slight change in the
Fig. 9). This can be caused

by a solvent effect on the evolution of radical pair structure. Spin polarization generated by the RPM will increase with increasing lifetime of the radical pairs. Hence, the strong increase in signal intensity observed on increasing solvent viscosity (Fig. 10) is consistent with the attribution of the spin polarization to the two RPM mechanisms.

As shown in Fig. 11, the polarization patterns in the spectra given by $CH_3^\bullet$ and $CD_3^\bullet$ formed by photolysis of IV-$CH_3$ and IV-$CD_3$ in toluene also exhibit a strong excitation wavelength ($\lambda_{ex}$) dependence [17]. Irradiation into the lowest-energy absorption band ($\lambda_{ex}$ = 440 and 532 nm) of IV-$CH_3$ gives rise to an E*A pattern, while an EA* pattern is observed for shorter excitation wavelengths ($\lambda_{ex}$ = 308 and 355 nm). In the case of IV-$CD_3$, an EA* pattern changes into an

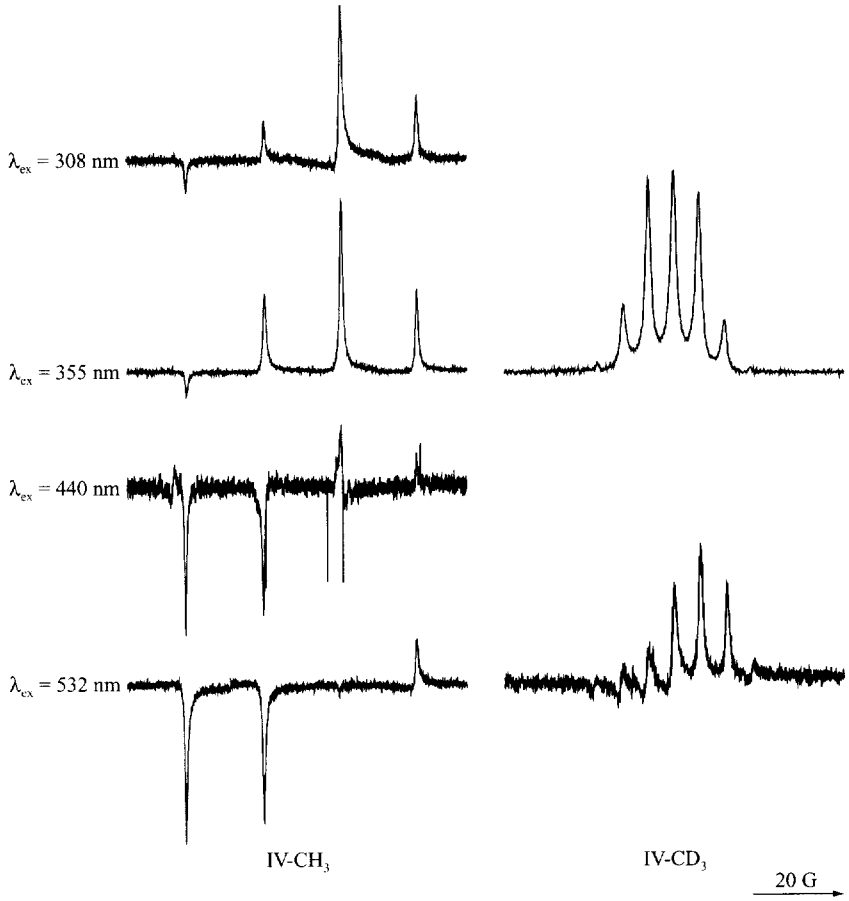


**Fig. 11.** Excitation wavelength dependence of the FTEPR spectra of methyl radicals produced by photoexcitation of about $2 \cdot 10^{-3}$ M solutions of [$Ru(SnPh_3)(CH_3)(CO)_2$(iPr-DAB)] (IV-$CH_3$) and [$Ru(SnPh_3)(CD_3)(CO)_2$(iPr-DAB)] (IV-$CD_3$) in toluene at room temperature. Delay time of 50 ns, absorption peaks point up. Excitation wavelengths are given in the figure.

A pattern. This striking effect is attributed to a $\lambda_{ex}$-dependent reaction pathway. It is in accordance with the finding that the photochemical reactions occur on a very short timescale and hence not necessarily from the thermally relaxed lowest excited state. The CIDEP patterns resulting from photolysis of solutions of compounds III and V do not show an excitation wavelength dependence. DFT-MO calculations have been used to determine the likely character and energy of the ground and first few excited states of IV-$CH_3$ and V. Results of these calculations offer a plausible explanation for the presence of a $\lambda_{ex}$ effect in the case of IV-$CH_3$ and the absence of an effect for V [17].

## 5 Concluding Remarks

The number of applications of TREPR in the field of transition-metal complexes photochemistry is still relatively small. Even so, it has been shown that this spectroscopic technique can make valuable contributions in this area of research. TREPR makes it possible to identify transient free radical intermediates through characteristic hyperfine coupling constants and $g$-values. In addition, information is obtained on precursor excited states and radical pairs involved in the radical formation process through CIDEP effects. In general, this information cannot be obtained with other spectroscopic techniques.

The work reviewed here shows that the interpretation of CIDEP effects is much more complex than in the case of free radical formation in organic photochemistry. In many of the applications discussed here, a definitive interpretation of spin polarization effects in terms of reaction mechanisms requires further studies. The complexity stems from the fact that the character of the electronic states that are involved in the photochemical reactions, in general, is less well defined, shows a wider variety than in the case of organic molecules, and can change significantly upon relatively minor changes in metal ion coordination environment.

The studies of the Co-, Ru-, Re-, and Pt-complexes illustrate the remarkably strong effects of solvent polarity, viscosity, and coordination ability on CIDEP patterns [16–20] and it is clear that the data contain much mechanistic information. The work on the Ru-, Re-, and Pt-complexes demonstrates that application of TREPR in this field of chemistry will be most productive when done in conjunction with detailed transient optical studies (UV, Vis, IR) and high-level computational work.

So far, TREPR studies have been confined to photoinduced bond homolysis reactions. However, application in studies of photoinduced electron transfer reactions involving transition-metal complexes can be envisaged as well and should be of interest.

## Aknowledgements

Financial support for this work was provided by the Division of Chemical Sciences, Office of Basic Energy Sciences, U.S. Department of Energy (DE-FG02-



84ER-13242), the Nethe
Netherlands Organization
and the Argentinean Agen
D.M.M. is member of th

1. Trifunac A.D., Lawler R.G
2. Bowman M.K. in: Modern
man M.K., eds.), pp. 1–42.
3. McLauchlan K.A. in: Mode
Bowman M.K., eds.). pp. 2
4. Hirota N., Yamauchi S. in:
pp. 187–248. New York: W
5. Hoff A.J. (ed.): Advanced
1989.
6. Kevan L., Bowman M.K. (
New York: Wiley 1990.
7. Weil J.A., Bolton J.R., We
8. Gorcester J., Millhauser G.
chemistry (Hoff A.J., ed.),
9. Schweiger A.: J. Chem. Sc
10. van Willigen H., Levstein
11. van Willigen H. in: Applic
Molecular and Supramolecu
197–247. New York: Marc
12. Salikov K.M., Molin Y.N.,
Effects in Radical Reaction
13. Hore P.J. in: Advanced EPR
440. Amsterdam: Elsevier
14. Sakaguchi Y., Hayashi H.,
15. Bussandri A., Kiarie C.W.,
16. Kleverlaan C.J., Martino D
18607 (1996)
17. van Slageren J., Martino D
Phys. Chem. A **104**, 5969
18. Kleverlaan C.J., Martino D
Magn. Reson. **15**, 203 (19
19. Kleverlaan C.J., Stufkens D
H., Vlček A. Jr.: J. Am. C
20. van Slageren J., Hartl F., S
309 (2000)
21. McLauchlan K.A., Yeung M
62. London: Royal Society
22. Clancy C.M.R., Tarasov V.
nance, pp. 50–78. London:
23. Levanon H., Möbius K.: A
24. Forbes M.D.E., Peterson J.
25. Massoth R.J.: Ph.D. thesis,
26. Derome A.E.: Modern NMR
27. Prisner T., Dobbert O., Di
28. Adrian F.: J. Chem. Phys.
29. Wong S.K., Hutchinson D.
30. Atkins P.W., Evans G.T.: M

84ER-13242), the Netherlands Foundation for Chemical Research (SON), the Netherlands Organization for the Advancement of Fundamental Research (NWO) and the Argentinean Agency for Scientific and Technologic Promotion (ANPCyT). D.M.M. is member of the Research Career of CONICET.

## References

1. Trifunac A.D., Lawler R.G., Bartels D.M., Thurnauer M.C.: Prog. React. Kinet. **14**, 43 (1984)
2. Bowman M.K. in: Modern Pulsed and Continuous-Wave Electron Spin Resonance (Kevan L., Bowman M.K., eds.), pp. 1–42. New York: Wiley 1990.
3. McLauchlan K.A. in: Modern Pulsed and Continuous-Wave Electron Spin Resonance (Kevan L., Bowman M.K., eds.). pp. 285–364. New York: Wiley 1990.
4. Hirota N., Yamauchi S. in: Dynamic Spin Chemistry (Nagakura S., Hayashi H., Azumiv T., eds.), pp. 187–248. New York: Wiley 1998.
5. Hoff A.J. (ed.): Advanced EPR: Applications in Biology and Biochemistry. Amsterdam: Elsevier 1989.
6. Kevan L., Bowman M.K. (eds.): Modern Pulsed and Continuous-Wave Electron Spin Resonance. New York: Wiley 1990.
7. Weil J.A., Bolton J.R., Wertz J.E.: Electron Paramagnetic Resonance. New York: Wiley 1994.
8. Gorcester J., Millhauser G.L., Freed J.H. in: Advanced EPR: Applications in Biology and Biochemistry (Hoff A.J., ed.), pp. 177–242. Amsterdam: Elsevier 1989.
9. Schweiger A.: J. Chem. Soc. Faraday Trans. **91**, 177 (1995)
10. van Willigen H., Levstein P.R., Ebersole M.H.: Chem. Rev. **93**, 173 (1993)
11. van Willigen H. in: Applications of Time-Resolved EPR in Studies of Photochemical Reactions, Molecular and Supramolecular Photochemistry (Schanze K.S., Ramamurthy V., eds.), chapt. 5, pp. 197–247. New York: Marcel-Dekker 2000.
12. Salikov K.M., Molin Y.N., Sagdeev R.Z., Buchachenko A.L.: Spin Polarization and Magnetic Effects in Radical Reactions (Molin Y.N., ed.). Amsterdam: Elsevier 1984.
13. Hore P.J. in: Advanced EPR: Applications in Biology and Biochemistry (Hoff A.J., ed.), pp. 405–440. Amsterdam: Elsevier 1989.
14. Sakaguchi Y., Hayashi H., I'Haya Y.: J. Phys. Chem. **94**, 291 (1990)
15. Bussandri A., Kiarie C.W., van Willigen H.: Res. Chem. Intermed. **28**, 697 (2002)
16. Kleverlaan C.J., Martino D.M., van Willigen H., Stufkens D.J., Oskam A.: J. Phys. Chem. **100**, 18607 (1996)
17. van Slageren J., Martino D.M., Kleverlaan C.J., Bussandri A., van Willigen H., Stufkens D.J.: J. Phys. Chem. A **104**, 5969 (2000)
18. Kleverlaan C.J., Martino D.M., van Slageren J., van Willigen H., Stufkens D.J., Oskam A.: Appl. Magn. Reson. **15**, 203 (1998)
19. Kleverlaan C.J., Stufkens D.J., Clark I.P., George M.W., Turner J.J., Martino D.M., van Willigen H., Vlček A. Jr.: J. Am. Chem. Soc. **120**, 10871 (1998)
20. van Slageren J., Hartl F., Stufkens D.J., Martino D.M., van Willigen H.: Coord. Chem. Rev. **208**, 309 (2000)
21. McLauchlan K.A., Yeung M.T.: Specialist Periodical Reports: Electron Spin Resonance, pp. 32–62. London: Royal Society 1994.
22. Clancy C.M.R., Tarasov V.F., Forbes M.D.E.: Specialist Periodical Reports: Electron Spin Resonance, pp. 50–78. London: Royal Society 1998.
23. Levanon H., Möbius K.: Annu. Rev. Biophys. Biomol. Struct. **26**, 495 (1997)
24. Forbes M.D.E., Peterson J., Breivogel C.S.: Rev. Sci. Instrum. **62**, 2662 (1991)
25. Massoth R.J.: Ph.D. thesis, University of Kansas, Lawrence, Kansas, USA, 1987.
26. Derome A.E.: Modern NMR Techniques for Chemistry Research. New York: Pergamon Press 1988.
27. Prisner T., Dobbert O., Dinse K.P., van Willigen H.: J. Am. Chem. Soc. **110**, 1622 (1998)
28. Adrian F.: J. Chem. Phys. **54**, 3918 (1971)
29. Wong S.K., Hutchinson D.A., Wan J.K.S.: J. Chem. Phys. **58**, 985 (1973)
30. Atkins P.W., Evans G.T.: Mol. Phys. **27**, 1633 (1974)

31. Freed J.H., Pedersen J.B.: Adv. Magn. Reson. **8**, 1 (1976)
32. Carrington A., McLachlan A.D.: Introduction to Magnetic Resonance, p. 201. New York: Harper & Row 1967.
33. Steiner U.E., Ulrich T.: Chem. Rev. **89**, 51 (1989)
34. Angerhofer A., Toporowicz M., Bowman M.K., Norris J.R., Levanon H.: J. Phys. Chem. **92**, 7164 (1988)
35. van Willigen H., Vuolle M., Dinse K.P.: J. Phys. Chem. **93**, 2441 (1989)
36. Levstein P.R., Ebersole M.H., van Willigen H.: Proc. Indian Acad. Sci.-Chem. Sci. **104**, 681 (1992)
37. Kottis P., Lefebvre R.: J. Chem. Phys. **39**, 393 (1963)
38. Ohara K., Hirota N., Martino D.M., van Willigen H.: J. Phys. Chem. A **102**, 5433 (1998)
39. Kaptein R., Oosterhoff L.: J. Chem. Phys. Lett. **4**, 214 (1969)
40. McLauchlan K.A., Stevens D.G.: J. Magn. Reson. **63**, 473 (1985)
41. Sekiguchi S., Kobori Y., Akiyama K., Tero-Kubota S.: J. Am. Chem. Soc. **120**, 1325 (1998)
42. Adrian F.J.: Chem. Phys. Lett. **272**, 120 (1997)
43. Shkrob I.A.: Chem. Phys. Lett. **264**, 417 (1997)
44. Bussandri A., van Willigen H.: Chem. Phys. Lett. **344**, 49 (2001)
45. Katsuki A., Akiyama K., Ikegami Y., Tero-Kubota S.: J. Am. Chem. Soc. **116**, 12065 (1994)
46. Steiner U., Haas W.: J. Phys. Chem. **95**, 1880 (1991)
47. Katsuki A., Akiyama K., Tero-Kubota S.: Bull. Chem. Soc. Jpn. **68**, 3383 (1995)
48. Sasaki S., Katsuki A., Akiyama K., Tero-Kubota S.: J. Am. Chem. Soc. **119**, 1323 (1997)
49. Sasaki S., Kobori Y., Akiyama K., Tero-Kubota S.: J. Phys. Chem. A **102**, 8078 (1998)
50. Khudyakov I.V., Serebrennikov Y.A., Turro N.J.: Chem. Rev. **93**, 537 (1993)
51. Ohtani M., Ohkoshi S., Kajitani M., Akiyama T., Sugimori A., Yamauchi S., Ohba Y., Iwaizumi M.: Inorg. Chem. **31**, 3873 (1992)
52. Ohkoshi S., Ohba Y., Iwaizumi M., Yamauchi S., Ohkoshi-Ohtani M., Tokuhisa K., Kajitani M., Akiyama T., Sugimori A.: Inorg. Chem. **35**, 4569 (1996)
53. Grissom C.B.: Chem. Rev. **95**, 3 (1995)
54. Walker L.A. II, Jarret J.T., Anderson N.A., Pullen S.H., Matthews R.G., Sension R.J.: J. Am. Chem. Soc. **120**, 3597 (1998)
55. Shiang J.J., Walker L.A. II, Anderson N.A., Cole A.G., Sension R.J.: J. Phys. Chem. B **103**, 10532 (1999)
56. Yoder L.M., Cole A.G., Walker L.A. II, Sension R.J.: J. Phys. Chem. B **105**, 12180 (2001)
57. Cole A.G., Yoder L.M., Shiang J.J., Anderson N.A., Walker L.A. II, Holl M.M.B., Sension R.J.: J. Am. Chem. Soc. **124**, 434 (2002)
58. Fessenden R.W., Schuler R.H.: J. Chem. Phys. **39**, 2147 (1963)
59. Babior B., Moss T.H., Orme-Johnson W.H., Beinert H.: J. Biol. Chem. **249**, 4537 (1974)
60. Baumgarten M., Lubitz W., Winscom C.J.: Chem. Phys. Lett. **133**, 102 (1987)
61. Boas J.F., Hicks P.R., Pilbrow J.R.: J. Chem. Soc. Faraday Trans. **73**, 417 (1977)
62. Bartels D.M., Lawler R.G., Trifunac A.D.: J. Chem. Phys. **83**, 2686 (1995)
63. Giannotti C., Bolton J.R.: J. Organomet. Chem. **80**, 379 (1974)
64. Arcos T., de Castro B., Ferreira M.J., Rangel M., Raynor J.B.: J. Chem. Soc. Dalton Trans. **1994**, 369.
65. Schrauzer G.N.: Inorg. Synth. **11**, 66 (1968)
66. Kleverlaan C.J., Stufkens D.J.: Inorg. Chim. Acta **284**, 61 (1999)
67. Turki M., Daniel C., Záliš S., Vlček A. Jr., van Slageren J., Stufkens D.J.: J. Organometallic Chem. **670**, 137 (2003)
68. Rossenaar B.D., Kleverlaan C.J., van de Ven M.C.E., Stufkens D.J., Vlček A. Jr.: Chem. Eur. J. **2**, 228 (1996)
69. Rossenaar B.D., Kleverlaan C.J., Stufkens D.J., Oskam A.: J. Chem. Soc. Chem. Commun. **1994**, 63.
70. Nieuwenhuis H.A., Stufkens D.J., Oskam A.: Inorg. Chem. **33**, 3212 (1994)
71. Nieuwenhuis H.A., van de Ven M.C.E., Stufkens D.J., Oskam A., Goubitz K.: Organometallics **14**, 780 (1995)
72. Aarnts M.P., Stufkens D.J., Wilms M.P., Baerends E.J., Vlček A. Jr., Clark I.P., George M.W., Turner J.J.: Chem. Eur. J. **2**, 1556 (1996)
73. van Slageren J., Klein A., Záliš S., Stufkens D.J.: Coord. Chem. Rev. **219–221**, 967 (2001)



74. van Slageren J., Hartl F., S
75. Aarnts M.P., Stufkens D.J.,
76. Farrell I.R., Matousek P., K
77. Lendzian F., Jaegerman P.,

**Authors' address:** Hans van V
ton, Boston, MA 02125, USA

74. van Slageren J., Hartl F., Stufkens D.J.: Eur. J. Inorg. Chem. 847 (2000)
75. Aarnts M.P., Stufkens D.J., Vlček A. Jr.: Inorg. Chim. Acta **266**, 37 (1997)
76. Farrell I.R., Matousek P., Kleverlaan C.J., Vlček A. Jr.: Chem. Eur. J. **6**, 1386 (2000)
77. Lendzian F., Jaegerman P., Möbius K.: Chem. Phys. Lett. **120**, 195 (1985)

**Authors' address:** Hans van Willigen, Chemistry Department, University of Massachusetts at Boston, Boston, MA 02125, USA